AD NUMBER

AD819198

NEW LIMITATION CHANGE

TO

Approved for public release, distribution unlimited

FROM

Distribution authorized to U.S. Gov't. agencies only; Administrative/Operational Use; AUG 1967. Other requests shall be referred to Army Electronics Command, Fort Monmouth, NJ.

AUTHORITY

USAEC ltr, 15 Jul 1969

AD 819198

Research and Development Technical Report
ECOM-02373F

INVESTIGATION OF
GENERAL WIRE ANTENNAS

FINAL REPORT

BY
M. G. ANDREASEN --- R. L. TANNER

AUGUST 1967

ECOM

UNITED STATES ARMY ELECTRONICS COMMAND · FORT MONMOUTH, N.J.

CONTRACT DA 28-043 AMC-02373(E)

TRG, DIVISION OF CONTROL DATA CORPORATION
535 BROAD HOLLOW ROAD
MELVILLE, NEW YORK 11746

NOTICES

INVESTIGATION OF GENERAL WIRE ANTENNAS

FINAL REPORT

May 1966 to July 1967

CONTRACT NO. DA 28-043 AMC-02373(E)

Prepared by

M. G. Andreasen and R. L. Tanner

TRG/Division of Control Data Corporation
Melville, New York

For

U. S. Army Electronics Command, Fort Monmouth, New Jersey

DISTRIBUTION STATEMENT

ABSTRACT

Integral equations for the current distribution on an arbitrary wire antenna have been programmed for a digital computer. The resulting computer program will calculate the current distribution, the input impedance, and the radiation pattern of a wire antenna of arbitrary geometry. Considered as a transmitting antenna, the antenna is excited by electromotive forces applied in any number of gaps along the wires. The program developed will permit these gaps to be connected by an arbitrary non-radiating network, and it will take into account resistive and reactive loading along the wires. The program will also treat the antenna as a receiving antenna, if desired, and then uses a distant dipole as the source of the induced current distribution. The numerical integral equation method used is essentially an exact method. The principal errors in the calculations arise in the numerical integration of the integrals in the integral equations, and these errors can be controlled. It is usually quite easy to obtain accuracies far better than normal measurement accuracies, and at a much lower cost.

Numerical results are presented for a simple dipole, a Yagi antenna array, a log-periodic antenna array, an airplane tail-cap antenna, a center-fed whip antenna, and a compact VHF antenna. Most results have been verified by measurements.

TABLE OF CONTENTS

LIST OF ILLUSTRATIONS

v

LIST OF ILLUSTRATIONS   (cont)

vi

LIST OF TABLES

1. INTRODUCTION

Most theoretical methods available today for calculating the
current distribution, the input impedance, and the radiation pattern
of wire antennas are of rather limited accuracy. Most methods are
not concerned with an evaluation of the current distribution but use,
rather, an assumed current distribution for calculating the radiation
pattern and the input impedance. The simple electrical dipole is the
only wire antenna for which, to the knowledge of the authors, attempts
have been made to calculate the current distribution with high accuracy.
Unfortunately, however, the analytical methods used to calculate the
current distribution on dipoles are not generally applicable to a wire
antenna of arbitrary configuration. The reason for this is to be found
in the limitations of the so-called analytical methods. For many years
the application of mathematical analysis has been the only method that
could be used to attempt the solution of electromagnetic boundary-
value problems. Today, with the existence of fast digital computers,
this is no longer true. Numerous problems that used to be considered
unsolvable, or for which only approximate solutions could be obtained,
can, in fact, be solved today in great generality and with high accuracy.
The general wire antenna is one such problem.

Before describing the method presented in this report to solve
the general wire antenna problem, we shall give a brief account of the
most important analytical methods that have been used to calculate
antenna impedance. The best known, and also the simplest, analytical
methods for calculating the input impedance of a wire antenna make
use of an assumed distribution of current on the antenna. By the
Poynting-vector method, one calculates the radiated power by inte-
grating the far-zone field of the assumed current distribution. The
input resistance of the antenna is then the ratio between the radiated
power and the square of the input current. The Poynting-vector method
was used by Hertz[1] as early as 1888 for calculating the power radiated
by a Hertzian dipole.

Since the Poynting-vector method uses only the far-zone field
for the impedance calculation, this method can give no information on
the antenna reactance which is associated with energy stored in the im-
mediate vicinity of the antenna. This disadvantage is avoided in the emf-
method which uses the near-zone field for the impedance calculation.
The emf-method also uses an assumed current distribution on the antenna.
This current distribution radiates a tangential electric field at the sur-
face of the antenna. The electric field, together with the known magnetic
field at the wire surface, represents a flow of complex power normal to
the wire surface. This complex power is used to define the antenna im-
pedance. For the true current distribution there is, of course, no flow
of power normal to the wire surface except at the gap where the emf
exciting the antenna is inserted. The accuracy of the Poynting-vector
method and of the emf-method depends upon the accuracy of the assumed

1

current distribution. As one might expect, the accuracy is usually much poorer for the reactance than for the resistance because the reactance depends much more strongly on the near-zone field than does the resistance. The accuracy usually is reasonably good for thin, resonant dipoles for which the current distribution can be predicted with good accuracy. The accuracy is not very good for general wire antennas, because the current distribution cannot be predicted with the required precision. The emf-method was originally developed by Brillouin[2] in 1922.

Both the Poynting-vector method and the emf-method make use of an assumed current distribution in the calculation of the antenna impedance. The first attempt to obtain a more accurate expression for the impedance by actually solving for the current distribution on a wire antenna was made by Hallén[3] who derived an integral equation for the current on a thin cylindrical dipole. Hallén's analytical solution of this integral equation has been improved by an iteration procedure and gives acceptable results for a thin dipole.

By considering the dipole to be a spherical transmission line, Schelkunoff[4,5] could express the total field around a dipole as a sum of spherical modes. For a dipole of arbitrary shape, these modes are coupled and the solution for the mode amplitudes satisfy an infinite set of coupled differential equations. For the thin dipole, certain approximations are possible because the principal spherical TEM-mode is excited much more strongly than other modes, and a reasonably accurate expression for the input impedance can be obtained. In the special case of a biconical antenna, an analytical solution can be obtained because the principal mode coupling occurs over a limited region near the ends of the antenna.

The development of the Schwinger variational principle during World War II has enabled the approximate solution of numerous complicated electromagnetic boundary-value problems. The cylindrical dipole is among the problems of practical interest that have been treated by this method. Using Hallén's integral equation for the current distribution on a cylindrical dipole, Tai[6] derived a variational expression for the input impedance. Tai showed that the assumption of a simple standing wave of current on the dipole leads to the same impedance as the emf method. More accurate results could be obtained by using more complex current distributions.

A review of the last eighty years of progress in analytical work on the linear antenna has been given by R. W. King.[7]

The limitations of the analytical method described above can be overcome by solving the integral equations for the antenna current

2

distribution directly by numerical techniques. This approach has been used by Mei[8] to solve a voltage-type integral equation (derivable from a voltage, analogous to Hallén's integral equation) for the current distribution on a wire antenna of arbitrary geometry. Mei presented numerical results for the current distribution on dipole, loop, and spiral antennas. Similar, but less general, techniques have been used by Baghdasarian and Angelakos[9] to calculate the current distribution on loop antennas, and by Richmond[10] to calculate the scattering from a straight wire. Most recently, Harrington[11] has solved an electric-type integral equation for the current distribution on a wire antenna. Harrington presented numerical results for a dipole.

Neither the voltage-type integral equation nor the electric-type integral equation are ideally suited for numerical calculations. The voltage-type integral equation does treat sources and sinks along the antenna with good accuracy, but, because it involves a double integration over the antenna, it is more complicated than the electric-type integral equation. On the other hand, the electric-type integral equation from which the current distribution can be found subject to conditions on the electric field along the wire surface, is not very convenient to use near sources and sinks where the tangential electric field will vary quite rapidly. In the present report, these difficulties have been overcome by using a combination of an electric-type and a voltage-type integral equation. The electric-type integral equation is used to satisfy the boundary conditions for the electric field at the surface of the wire composing the antenna (excluding the gaps). At the gaps of the antenna where sources or sinks may be located, a voltage-type equation is satisfied.

As shown in Fig. 1, the wire antenna considered in this report may contain an arbitrary number of gaps, all of which can be coupled together by an arbitrary non-radiating network; e.g., by transmission lines as they are used in log-periodic antennas. When the antenna gaps are coupled by a network, the gap conditions also become coupled equations in the gap currents.
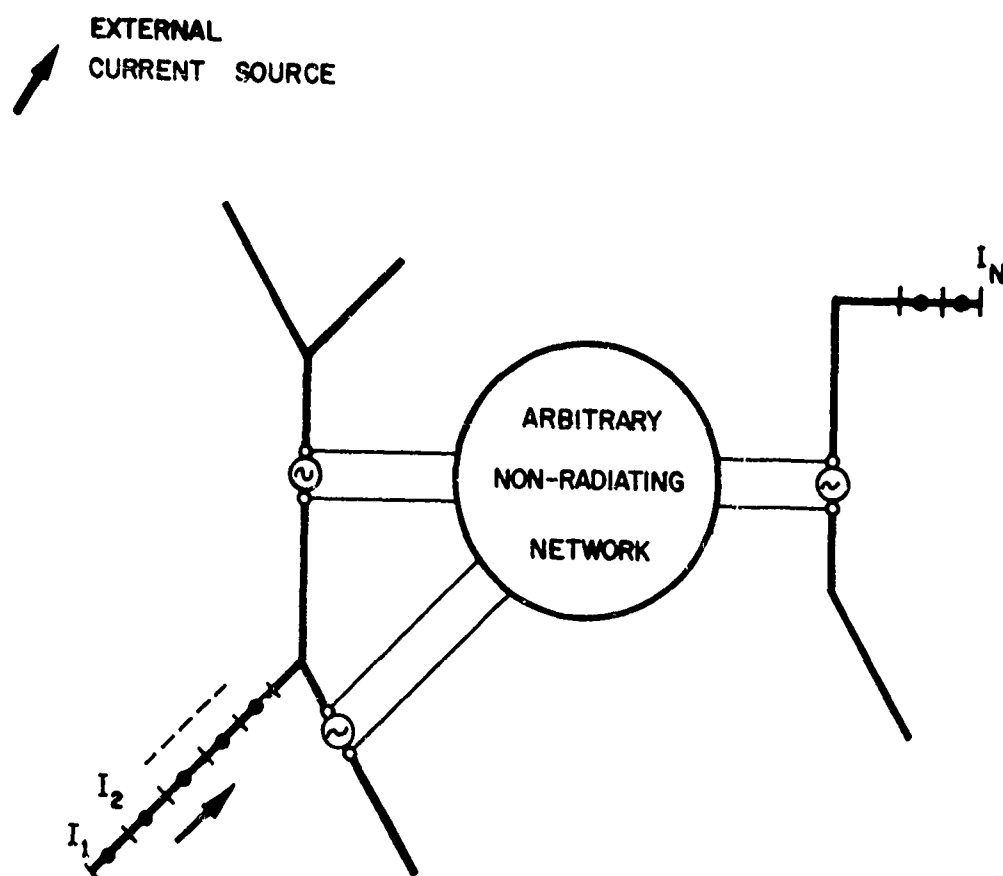
EXTERNAL
CURRENT SOURCE

Fig. 1   Arbitrary Wire Antenna

4

2. METHODS OF CHECKING THE ACCURACY

When one develops a computer program to calculate the proper-
ties of virtually any wire antenna with very high accuracy, it is im-
portant to be able to check out the program by comparison with results
that have been obtained by other methods. The only theoretical case
for which a comparison is worth while is the simple dipole antenna.
In most cases one must, therefore, rely on experimental measurements
for a comparison. The quantity best suited for a comparison is the in-
put impedance of the antenna. The input impedance describes an impor-
tant property of the antenna in terms of only two numbers -- a resistance
and a reactance. From an experimental point of view, the input im-
pedance can be determined with much higher accuracy than either the
current distribution or the radiation pattern of the antenna. Also, from
a theoretical point of view, it is known that the input impedance calcu-
lated at the gaps of a wire antenna will often depend quite critically
upon the accuracy of the current distribution while the radiation pattern
is usually less sensitive to small errors in the current distribution.
The thin center-fed half-wave dipole is an excellent example of this
fact. The current distribution most often used on this dipole is of
sinusoidal form -- a distribution which is extremely close to the cor-
rect form and which will also permit the radiation pattern to be cal-
culated with high accuracy. However, the input impedance, which is
proportional to the derivative of the current at the gap, is zero when
the current distribution is assumed to be sinusoidal. The current dis-
tribution and radiation pattern will, therefore, often be calculated with
much higher accuracy than the input impedance.

From the foregoing discussion, we conclude that the input im-
pedance will often be better suited for checking calculations than either
the current distribution or the radiation pattern. This may not be true
in cases where parts of the antenna are very weakly coupled to the input
terminals of the antenna and where, therefore, the current distribution
could conceivably possess errors that would not show up very strongly
in the input impedance. Such errors, if present, would of course affect
the accuracy of the radiation pattern. Whether such errors are present
or not can be determined by calculating the radiation resistance of the
antenna by the Poynting-vector method: integrating the radiation pattern
over all directions of space. If the radiation resistance thus obtained
does not agree with the resistance calculated at the input terminals of
the antenna, the errors mentioned are probably present. Most of the
numerical results presented in this paper are input impedance data.

When the antenna is considered as a transmitting antenna, the
source of the current distribution induced in a wire antenna is, of course,
emf's introduced at various places in the antenna. Quite often, however,
the antenna is considered a receiving antenna, and the problem is now

5

to calculate the current distribution induced in the wire antenna by an incident plane wave, and to calculate the scattering pattern of the receiving antenna. The source is, in this case, the incident plane wave. The computer program developed for the general wire antenna accepts both types of sources.

3. THE INTEGRAL EQUATIONS FOR ARBITRARY WIRE ANTENNAS

The electromagnetic field radiated by a wire antenna is given in terms of an integral transform of the current distribution. Therefore, the evaluation of the radiation field is, in general, a simple matter once the current distribution is known. The current distribution on the antenna is correct when the electric field it radiates has zero tangential components on all metallic surfaces on the antenna and when the current distribution in the gaps satisfies certain conditions to account for the sources and sinks placed there. Satisfying these boundary conditions at the antenna surface and in the gaps leads to an integral equation for the current distribution, which we shall now derive.

The time factor $e^{j\omega t}$ and m.k.s. units will be used throughout the report.

The electric field vector $\overline{\overline{E}}$ produced by a current density distribution $\overline{J}$ in free space can be expressed as a volume integral over the source distribution

$$\overline{E}(\overline{r}') = - \frac{j\omega\mu}{4\pi} k \int_V \overline{J}(\overline{r}) \cdot \overline{\overline{G}}(\overline{r}, \overline{r}') \, dv. \tag{1}$$

Here, $\overline{r}'$ is the radius vector of the observation point, and $\overline{r}$ is the radius vector of the source point. The function $\overline{\overline{G}}$ is a dyadic which, according to Silver,[12] is given by

$$\overline{\overline{G}}(\overline{r}, \overline{r}') = \left[f_1(kR)\hat{R}\hat{R} + f_2(kR)\hat{\overline{\overline{\epsilon}}} \right] \frac{e^{-jkR}}{kR} \tag{2}$$

where $k = 2\pi/\lambda$ is the free space propagation constant. R is the distance from the source point to the observation point, $\hat{R}$ is a unit vector pointing from the observation point to the source point (see Fig. 2), and $\hat{\overline{\overline{\epsilon}}}$ is the unit dyad. The functions f_1 and f_2 are defined as follows:

$$f_1(x) = -1 + j\frac{3}{x} + \frac{3}{x^2}. \tag{3}$$

$$f_2(x) = 1 - j\frac{1}{x} - \frac{1}{x^2}. \tag{4}$$

Let us apply Eq. (1) to a wire antenna. In a wire antenna, the current flows on the surface of wires. For simplicity, we shall assume in the following that the current flows on the axis of the wire. The relative error thereby introduced in calculations of the electric field on the wire surface is of the order of

$$1 - J_0(kr_0) \approx \frac{1}{2}(kr_0)^2 \quad \text{where} \quad r_0 \text{ is the wire radius.}$$

For most practical purposes, this error is negligible. Correction terms compensating for this error could be derived, if necessary.

Assuming the current vector on the axis of the wire to be $\bar{I}(\bar{r})$, Eq. (1) reduces to the following line integral over the axes of the wire structure

$$\bar{E}(\bar{r}') = -\frac{j\omega\mu}{4\pi}\int_C I(t)\,\hat{i}(t)\cdot\bar{\bar{G}}(\bar{r},\bar{r}')\,d(kt) \tag{5}$$

where t is a coordinate measured along the wire, $I(t)$ is the current flowing, and $\hat{i}(t)$ is the unit vector in the defined positive direction of current flow at the coordinate t (see Fig. 2). The integration is extended over the entire wire structure. When Eq. (2) for $\bar{\bar{G}}$ is introduced in this equation, we obtain

$$\bar{E}(\bar{r}') = -\frac{j\omega\mu}{4\pi}\int_C I(t)\left[f_1(kR)\hat{i}(t)\cdot\hat{R}\hat{R} + f_2(kR)\hat{i}(t)\right]\frac{e^{-jkR}}{kR}\,d(kt). \tag{6}$$

To arrive at the integral equation for the current distribution $I(t)$, we shall now satisfy the boundary condition for the tangential electric field at the surface of the wire. We shall assume that the source of the current distribution induced on the wire structure includes an external source which radiates a wave incident on the antenna with the electric field vector $\bar{E}^{inc}(t')$ at coordinate t' of the antenna. The boundary condition at the surface of the wire requires that the total tangential electric field equal the product of the internal wire impedance per unit length Z^W and the current flowing in the wire. The total field at the wire surface is the sum of the incident field and the field expressed by Eq. (6). We find, therefore, the following integral equation for the current distribution $I(t)$
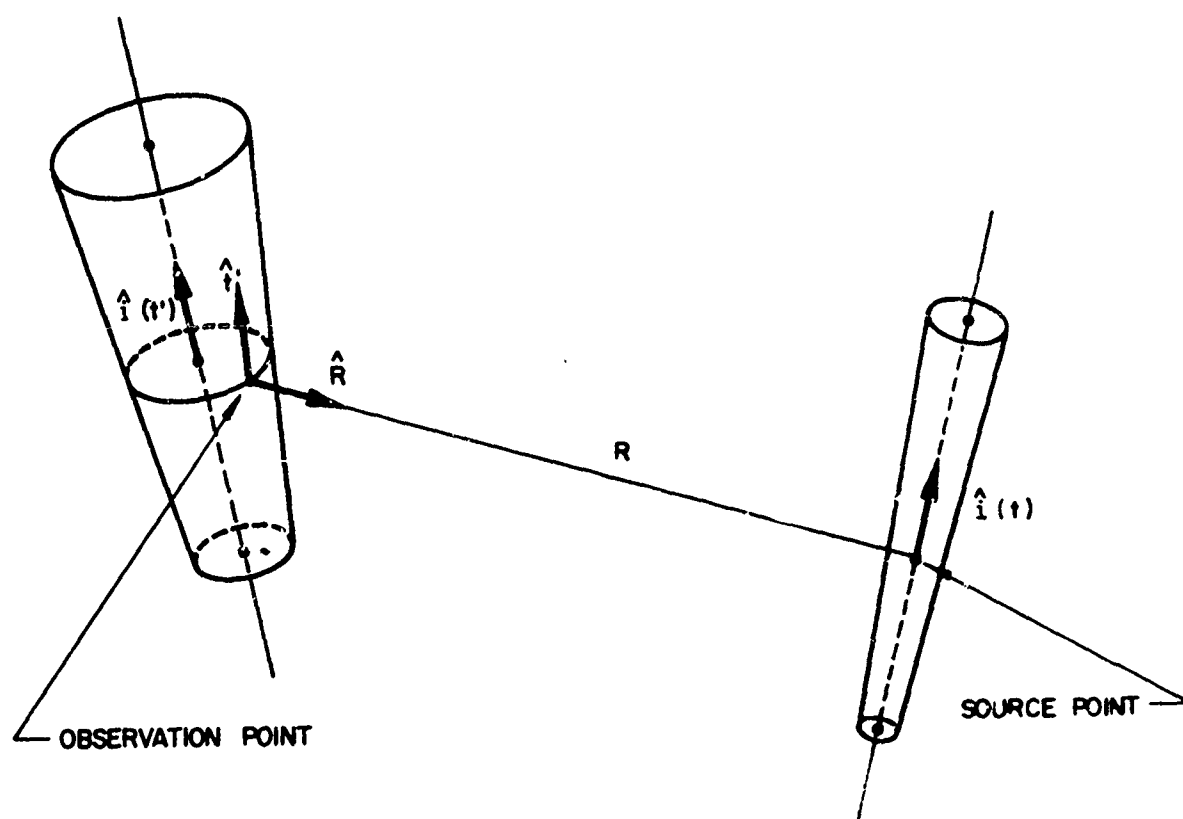
8

$\hat{1}$ (t') $\hat{1}$

$\hat{R}$

R

$\hat{1}$ (t)

OBSERVATION POINT

SOURCE POINT

Figure 2.   Symbols Used at Source and Observation Points

9

$$\hat{t}' \cdot \overline{E}^{inc}(t') = Z^W(t') I(t') + \frac{j\omega\mu}{4\pi} \hat{t}' \int I(t)\left[f_1(kR)\hat{i}(t)\cdot\hat{R}\hat{R} + f_2(kR)\hat{i}(t)\right]\frac{e^{-jkR}}{kR} d\{kt\}. \tag{7}$$

The observation point at which the boundary condition is satisfied has the coordinate t' measured along the wire structure and is located a distance from the wire axis equal to the wire radius at the point t', while $\hat{t}'$ is a unit vector pointing along the wire surface at the observation point ($\hat{t}'$ has no circumferential component to the wire), as shown in Fig. 2. We assume here that the wires composing the antenna are of conical shape. $\hat{t}'$ is therefore not necessarily identical to $\hat{i}(t')$ but does, in general, point in a different direction depending upon where the observation point is chosen along the wire perimeter. Strictly, Eq. (7) should hold for any point on the surface of the wire. However, the equation cannot be satisfied in all points along the circumference of the wire because we have tacitly neglected circumferential currents on the wires, an approximation which is extremely good in most practical cases and is, of course, better the thinner the wire is. Accordingly, it should make little difference where we choose the observation point on the wire circumference. Yet, having neglected the circumferential current component, we can sometimes do better than just choosing an arbitrary observation point on the wire circumference. Considering, for example, the incident field on the left-hand side of Eq. (7), it is more accurate to evaluate the field in the direction of the wire axis in an observation point placed on the wire axis itself than it is to evaluate the field in any point on the wire circumference. On the left-hand side of Eq. (7), we therefore replace $\hat{t}'$ by $\hat{i}(t')$ and tacitly assume the observation point to be on the wire axis. On the right-hand side of Eq. (7), we shall also replace $\hat{t}'$ by $\hat{i}(t')$ and assume the observation point to be on the wire axis rather than on the wire surface. We require, however, that the wire axis at the source point and the wire axis at the observation point do not coincide. If the wire axes do coincide, the observation point is chosen on the wire surface. Since the field radiated by the source is in that case symmetric about the wire axis, the observation point can be chosen anywhere on the wire circumference. Accordingly, on the right-hand side of Eq. (7), let us replace $\hat{t}'$ by a vector $\hat{s}'$ defined as follows

$$\hat{s}' = \begin{cases} \hat{i}(t') & \text{when } \hat{R} \times \hat{i}(t') \neq 0 \\[2ex] \hat{t}' & \text{when } \hat{R} \times \hat{i}(t') = 0. \end{cases} \tag{8}$$

10

Tacitly assuming the observation point to be chosen as described above, after a few transformations of Eq. (7) we arrive at the following integral equation for $I(t)$

$$\frac{1}{k}\hat{i}(t')\cdot \overline{E}^{inc}(t') = \frac{Z^w(t')}{k} I(t')$$

$$+ j30\,\hat{s}'\!\!\int_C I(t)\left[f_1(kR)\hat{i}(t)\cdot\hat{R}\hat{R}+f_2(kR)\hat{i}(t)\right]\frac{e^{-jkR}}{kR}\,d(kt). \qquad (9)$$

11

4. REDUCTION TO A SET OF LINEAR EQUATIONS

In order to obtain a solution of the integral equation, Eq. (9), we shall reduce it to a set of simultaneous linear equations in sampled values of the current distribution. Assume the total length of wire to be divided into N intervals. Let the sampled value of the current in the center point of the n'th interval Δ_n be I_n, and let the coordinate in that point be t_n (see Fig. 1). The integral in Eq. (9) can now be approximated by a linear combination of the N sampled currents, and these currents can be solved for by satisfying the integral equation (9) in the N sampling points. This leads to a set of N linear equations which can be solved by a digital computer. The accuracy of the solution will depend quite strongly upon how the reduction of the integral in Eq. (9) to a linear combination of the sampled current values is accomplished. It is important that the final current distribution, calculated to satisfy the boundary conditions correctly in the sampling points chosen, also produce a boundary field that varies smoothly between the sampling points. Otherwise, the boundary field which acts as a virtual emf that drives an erroneous current through the antenna, could significantly impair the accuracy of the solution. We have found that a constant or linearly varying current in each interval of the antenna, as used by Harrington,[11] can lead to significant errors when the interval length is much greater than the wire diameter. Instead, the following representation for the current distribution in the n'th interval of the antenna was found to lead to very satisfactory accuracy in most cases:

$$I(t) = T_n + C_n \cos\left[k(t - t_n)\right] + S_n \sin\left[k(t - t_n)\right] . \tag{10}$$

This distribution represents a sum of a constant current T_n and a standing wave with propagation constant of free space. This distribution has been used also by Mei.[8]

When Eq. (10) is introduced in the integral equation Eq. (9), and Eq. (9) is required to be satisfied in the N sampling points, we find, by integrating over the N integration intervals the following set of equations:

12

$$\frac{1}{k} \hat{i}_m \cdot \overline{E}_m^{inc} = \frac{z_m^w}{k} I_m + \sum_{n=1}^{N} \hat{s}_m \cdot \left[T_n \overline{G}_o\left(\overline{R}_{nm}, \hat{i}_n, \Delta_n\right) \right.$$

$$\left. + C_n \overline{G}_c\left(\overline{R}_{nm}, \hat{i}_n, \Delta_n\right) + S_n \overline{G}_s\left(\overline{R}_{nm}, \hat{i}_n, \Delta_n\right) \right] ; \, m = 1,2\text{-----},N \quad (11)$$

where $\hat{i}_m$, $\overline{E}_m^{inc}$, z_m^w, $\hat{s}_m$, and I_m are the values of $\hat{i}$, $\overline{E}^{inc}$, z^w, $\hat{s}$, and I at the m'th sampling point, and Δ_n is the length of the n'th integration interval. $\overline{R}_{nm}$ is the vector pointing from the n'th sampling point to the m'th observation point, and $\hat{i}_n$ is the value of $\hat{i}$ at the n'th sampling point.

The vector functions $\overline{G}_o$, $\overline{G}_c$, and $\overline{G}_s$ appearing in Eq. (11) represent the electric field radiated by a dipole of length Δ_n, oriented in the direction $\hat{i}_n$, and carrying a constant, cosine- or sine-distribution of current respectively. The field is evaluated in a point with radius vector $\overline{R}_{pm}$ pointing from the center of the dipole. The functions $\overline{G}_o$, $\overline{G}_c$, and $\overline{G}_s$ are derived in Appendix A.

As shown in Appendix B, the constants T_n, C_n, and S_n can be expressed as a linear combination of a maximum of three sampled values of current because a constant - cosine - sine curve can be fitted to three points only. When T_n, C_n, and S_n can be expressed as linear combinations of the current values in the N sampling points, Eq. (11) obviously can be interpreted as a set of N linear equations which can be solved for the N unknown sampled current values. If we consider the antenna as a transmitting antenna, however, the incident field $\overline{E}^{inc}$ is zero, and the solution of Eq. (11) is zero, eigensolutions of the equation being ignored. The reason why the solution turns out to be zero is obviously that we have not yet defined how we want to excite the antenna. An additional condition must be satisfied at each gap of the antenna. This gap condition can also be reduced to a linear combination of the sampled current values. However, for each gap condition added to Eq. (11), we have to introduce an extra unknown to keep the total number of unknowns the same as the total number of equations. The most natural choice for this unknown is the gap current itself. When gaps are present, some of the constants T_n, C_n, and S_n will also depend upon the gap currents. Assuming the presence of N_{gap} gaps, and numbering the gap currents from $N+1$ through $N+N_{gap}$, Eq. (11) can therefore be written in the following abbreviated form:

13

$$\sum_{n=1}^{N+N_{gap}} G_{mn} I_n = \frac{1}{k} \hat{i}_m \cdot \bar{E}_m^{inc} \; ; \quad m = 1, 2, \text{----}, N. \tag{12}$$

The gap conditions are quite complex in the general case where several wires join at the gap, where sources and/or sinks can be inserted into each wire of the junctions, and where all junctions can be connected by an arbitrary non-radiating network, as shown in Fig. 1. In order to understand the nature of the gap condition, we shall set up the condition in a simplified situation. Assume that each gap joins only two wires, and that these gaps are not connected by a network. Assume furthermore that the wires are conical near the gap (see Fig. 3). The dominant field near the gap can then be represented by a TEM-wave on a biconical transmission line, and the standard transmission line equations permit establishing the desired relationship between the current distribution and the source generating it. Accordingly, we find for the terminal voltage at the gap

$$j \, Z_o \, \frac{dI}{d(kt)} = V_i - Z_i I \tag{13}$$

where V_i is the generator emf, Z_i is the generator impedance, Z_o is the characteristic impedance of the biconical transmission line, and

$$\frac{dI}{d(kt)}$$

is the derivative of the current on the "positive" side of the gap $(t > t_g)$. Equation (13) is correct only if the current distribution is symmetric about the gap. This cannot, in general, be assumed to be the case. The current distribution will, therefore, in general also contain a first-order spherical mode near the gap. While this mode does not contribute to the gap current itself, it does contribute to the derivative of the current. Fortunately, however, the derivative of the TEM-wave is an odd function about the gap, while the first-order wave is an even function about the gap. The first-order wave can, therefore, be eliminated from Eq. (13) by replacing the derivative in Eq. (13) by half the difference between the derivatives on the two sides of the gap

$$j \, \frac{1}{2} Z_o \left[\left(\frac{dI}{d(kt)} \right)_{t > t_g} - \left(\frac{dI}{d(kt)} \right)_{t < t_g} \right] = V_i - Z_i I. \tag{14}$$

14
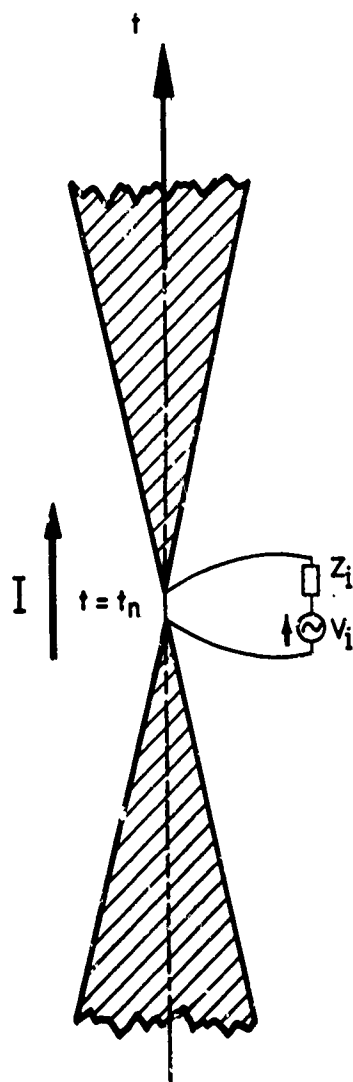
Fig. 3   Gap Region

The derivates in this equation can, of course, be approximated numerically quite well as a linear combination of a few of the sampled currents, including the gap current. Omitting the details of this calculation, we find that for N_{gap} gaps, Eq. (14) can be reduced to the following set of equations:

$$\sum_{n=1}^{N+N_{gap}} H_{mn} I_n = V_{im} \quad ; \quad m = N+1, N+2, \text{------}, N+N_{gap}. \quad (15)$$

where V_{im} is the emf in the gap numbered m.

Equations (12) and (15) form a set of $N+N_{gap}$ simultaneous linear equations from which the $N+N_{gap}$ unknown current values can be found. These equations can be solved by a digital computer. When the currents have been found, the input impedance of the antenna seen from the various gaps is, of course, immediately found as the ratio between the voltage across the gap and the gap current

$$Z_m^{input} = \frac{V_{im} - Z_{im} I_m}{I_m} \quad ; \quad m = N+1, N+2, \text{----}, N+N_{gap} \quad (16)$$

where Z_{im} is the generator impedance at the gap numbered m and I_m is the gap current.

16

5. THE RADIATION PATTERN

When the unknown currents have been found, it is, of course, also an easy matter to calculate the radiation pattern. The radiated far-zone field can be calculated basically from the same set of formulas derived in Appendix A, but these formulas can be simplified considerably when the observation point is in the far zone. Without going into the details of these calculations, we find the following expression for the electric field vector $\overline{E}$ in the far zone

$$\frac{1}{k}\overline{E} = j30 \frac{e^{-jkR}}{kR} \sum_{n=1}^{N} e^{jk\overline{R}_n \cdot \hat{R}} \left[T_n \overline{E}_{on} + C_n \overline{E}_{cn} + S_n \overline{E}_{sn} \right] \qquad (17)$$

where R is the distance from the origin of the coordinate system to the observation point in the far-zone, and $\hat{R}$ is a unit vector pointing in that direction. $\overline{R}_n$ is the radius vector of the center of the n'th interval of the antenna. $\overline{E}_{on}$, $\overline{E}_{cn}$, and $\overline{E}_{sn}$ have components in the direction of $\hat{i}_n$ and of the perpendicular unit vector

$$\hat{\rho}_n = \frac{\hat{R} - \left(\hat{R} \cdot \hat{i}_n\right)\hat{i}_n}{\left|\hat{R} - \left(\hat{R} \cdot \hat{i}_n\right)\hat{i}_n\right|} \qquad (18)$$

which is normal to $\hat{i}_n$.

For these components the following expressions are found:

$$\overline{E}_{on} \cdot \hat{i}_n = -2\left[1 - (\hat{R} \cdot \hat{i}_n)^2\right] \frac{\sin\left(\frac{k\Delta_n}{2} \hat{R} \cdot \hat{i}_n\right)}{\hat{R} \cdot \hat{i}_n} . \qquad (19)$$

$$\overline{E}_{on} \cdot \hat{\rho}_n = -\overline{E}_{on} \cdot \hat{i}_n \frac{\hat{R} \cdot \hat{i}_n}{\sqrt{1 - (\hat{R} \cdot \hat{i}_n)^2}} . \qquad (20)$$

$$\overline{E}_{cn} \cdot \hat{i}_n = -2\sin\left(\frac{k\Delta_n}{2}\right)\cos\left(\frac{k\Delta_n}{2} \hat{R} \cdot \hat{i}_n\right)$$

$$+ 2\cos\left(\frac{k\Delta_n}{2}\right)\sin\left(\frac{k\Delta_n}{2} \hat{R} \cdot \hat{i}_n\right)\hat{R} \cdot \hat{i}_n . \qquad (21)$$

17

$$\overline{E}_{cn} \cdot \hat{\rho}_n = -\overline{E}_{cn} \cdot \hat{i}_n \frac{\hat{R} \cdot \hat{i}_n}{\sqrt{1 - (\hat{R} \cdot \hat{i}_n)^2}} \cdot \tag{22}$$

$$\overline{E}_{sn} \cdot \hat{i}_n = j2 \cos\left(\frac{k\Delta_n}{2}\right) \sin\left(\frac{k\Delta_n}{2} \hat{R} \cdot \hat{i}_n\right)$$

$$- j2 \sin\left(\frac{k\Delta_n}{2}\right) \cos\left(\frac{k\Delta_n}{2} \hat{R} \cdot \hat{i}_n\right) \hat{R} \cdot \hat{i}_n \cdot \tag{23}$$

$$\overline{E}_{sn} \cdot \hat{\rho}_n = -\overline{E}_{sn} \cdot \hat{i}_n \frac{\hat{R} \cdot \hat{i}_n}{\sqrt{1 - (\hat{R} \cdot \hat{i}_n)^2}} \cdot \tag{24}$$

These expressions are easily evaluated by a digital computer. Since the input resistance of the antenna is already known, the absolute gain of the antenna can be calculated. The far-zone field will generally be elliptically polarized. The computer program developed calculates the gain along the two principal axes of the polarization ellipse, the total gain, the axial ratio, the orientation, and the sense of rotation of the polarization ellipse.

6. SYMMETRY CONSIDERATIONS

Often an antenna will possess certain symmetry properties such that only part of the total current distribution is unknown while the rest of the current distribution can be described in terms of the unknown current distribution (e.g., an antenna and its image in a perfect ground plane). A considerable amount of computer time can be saved by taking these symmetry properties into account and solving for only that part of the current distribution that is really unknown. In setting up the equations for the unknown current distribution, it is, of course, necessary to take the mutual coupling between the unknown current distribution and the rest of the current distribution properly into account.

The computer program developed will utilize the symmetry properties of an antenna and its image in a perfectly conducting ground plane, and will also utilize the symmetry properties of the azimuthal modes of a ring array of an arbitrary number of equispaced wire antennas.

7. NUMERICAL RESULTS

The computer program developed will solve for the current distribution, the input impedance, and the radiation pattern of virtually any ring antenna array whose basic element is a wire antenna of essentially arbitrary geometry. There is no basic limitation to the electrical size of the antenna that can be handled, but the cost of the calculations increases at a rate between the square and the cube of the electrical size. The maximum integration interval length that can be chosen depends upon geometry, but can seldom be allowed to exceed 0.25 wavelengths without a considerable loss of accuracy. When the matrix for the equations to be solved by the computer does not fit into the memory of the computer, part of the matrix will be on magnetic tape.

To illustrate the use of the computer program developed, we shall now show some numerical results obtained for a number of wire antennas. The results have, in most cases, been verified by measurements.

The only wire antenna that it has been possible to analyze with high accuracy by analytical methods is the simple dipole.[7, 13] Since the analytical results for the dipole are supposedly more accurate than most measured results, it is very valuable to be able to check the accuracy of the general computer program developed by comparison against the analytical results for a dipole. Table 1 shows the values of input impedance for a cylindrical dipole obtained by the second-order approximation method of King and Middleton.[13] The Table also shows the results obtained by the present computer program when the dipole is excited through a conical gap extending over ten percent of the length of the dipole. The agreement between the values of input resistance is seen to be extremely good. Some differences are observed in the reactance values, probably due to the fact that the dipole treated by the present program has a conical gap. The total number of integration intervals used for the calculations in Table 1 was 20. In most practical cases where the accuracy need not be nearly so high as in Table 1, many fewer intervals can be used.

In most cases, the computer program developed for calculating the properties of arbitrary wire antennas must be checked out by careful experimental measurements. Figures 4 through 12 show the calculated and measured input impedance of various wire antennas. Figures 4 and 5 show the input impedance of a fat monopole and of a fat conical monopole. The agreement between the theoretical and the experimental results is seen to be excellent.

20

Table 1.

Input Impedance of Linear Antenna above Perfect Ground

Antenna Height h.   Wire Radius a.

$$\Omega \;=\; 2 \cos \left(\frac{2h}{a} \right) = 15.$$

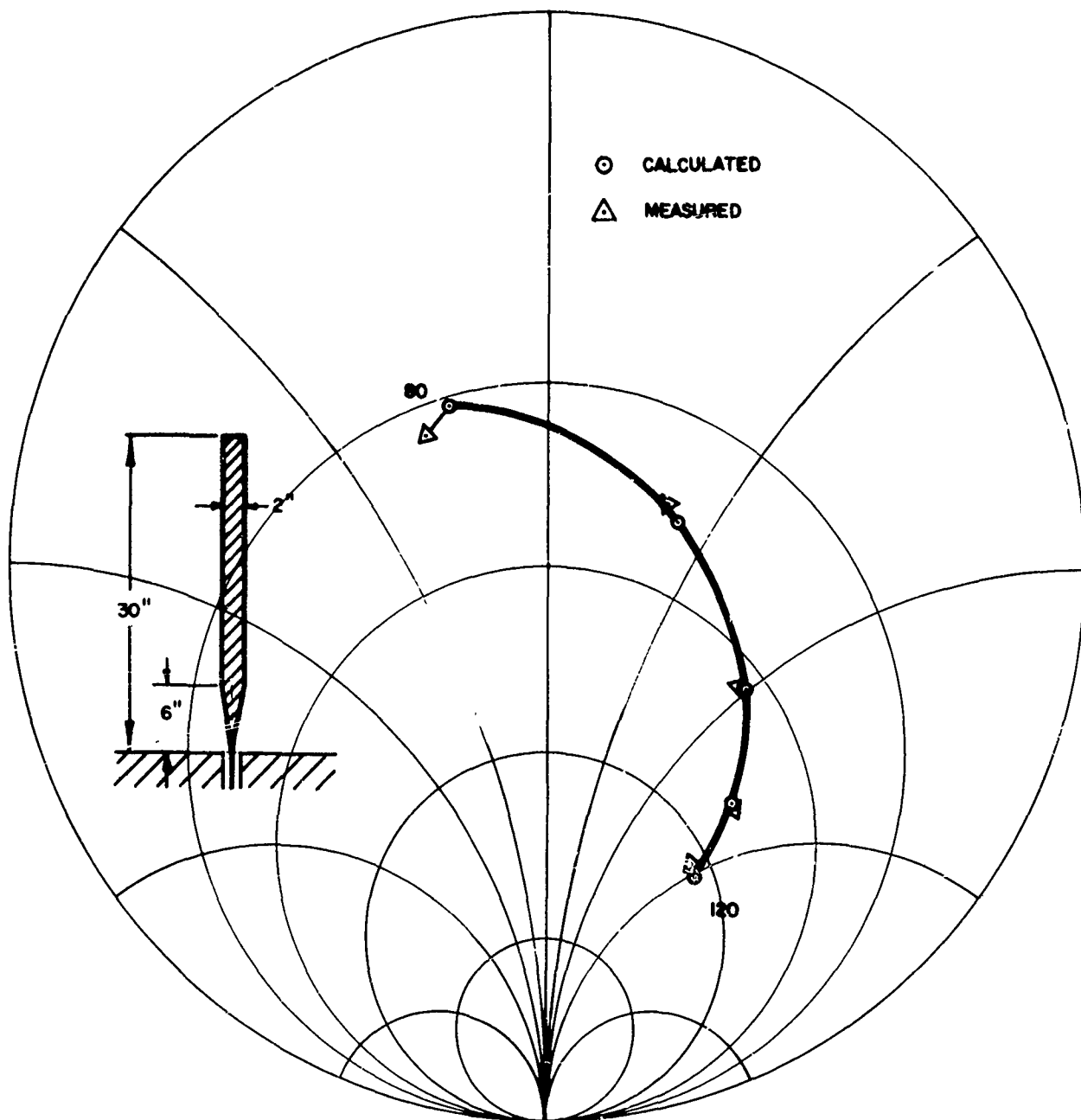|	Resistance, Ohms		Reactance, Ohms	
kh	Andreasen-Tanner	King-Middleton	Andreasen-Tanner	King-Middleton
0.5	2.46	2.50	- 639	- 628
0.7	5.14	5.14	- 409	- 405
0.9	9.07	9.07	- 266	- 267
1.1	14.8	14.7	- 162	- 165
1.3	22.9	22.8	- 75.1	- 81.8
1.5	34.9	34.7	3.9	- 5.1
1.7	53.0	52.9	82.2	71.4
1.9	81.5	82.5	166	155

Fig. 4.   Input Impedance of Fat Monopole above Ground from
         80 MHz to 120 MHz in Steps of 10 MHz
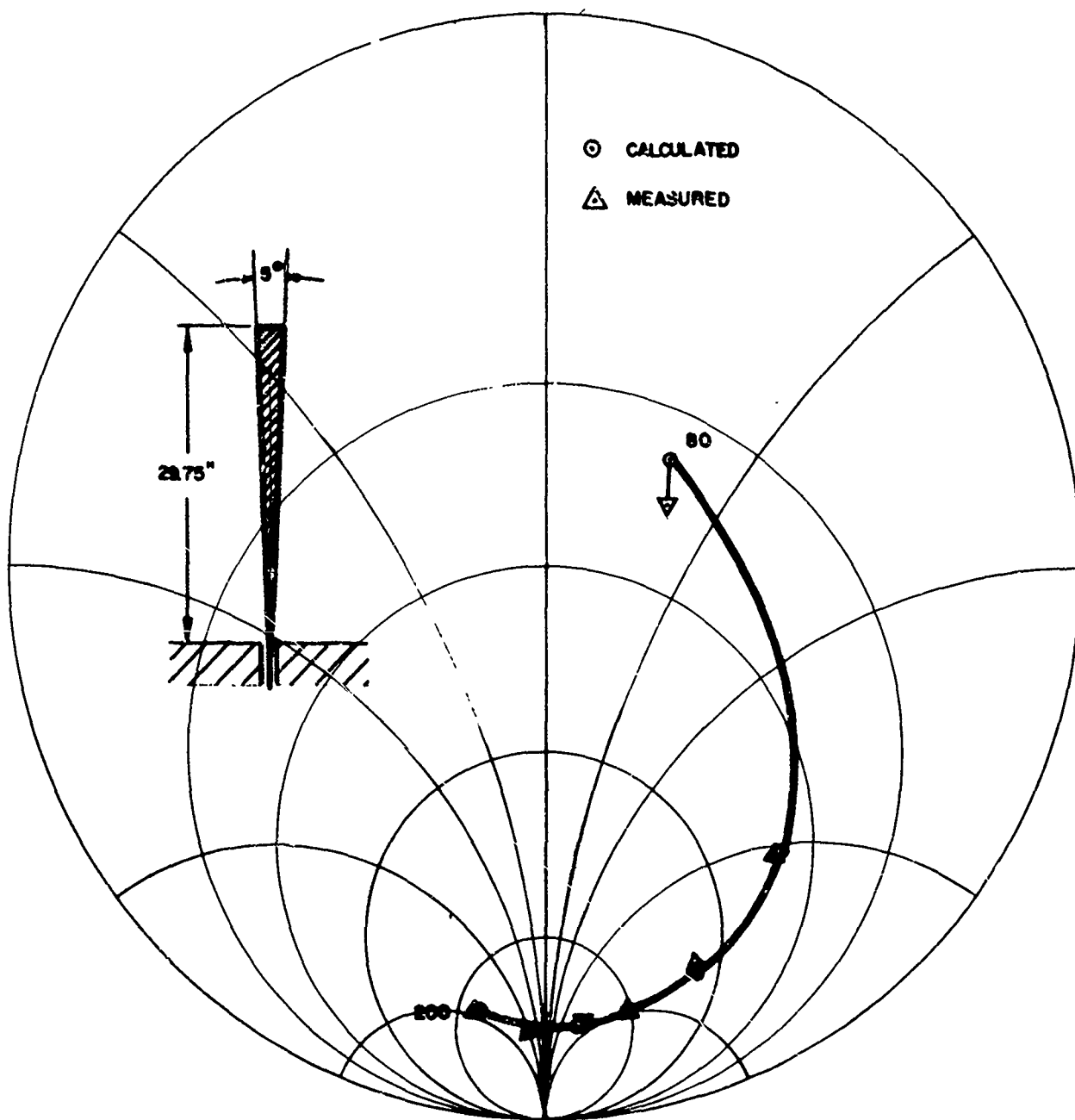   (Chart Impedance = 50 ohms)

22

Fig. 5. Input Impedance of Conical Monopole above Ground from 80 MHz to 200 MHz in Steps of 20 MHz (Chart Impedance = 50 ohms)

23

Figure 6 shows a 2.5 to 1 log-periodic array of five elements fed from a 200 ohm transmission line. The calculated and measured input impedance of this antenna over the 2.5 to 1 frequency band in which it should be operative is shown in Figs. 7 and 8. The agreement between the theoretical and the measured results is seen to be extremely good. Even the smaller loops of the impedance curve, which are due to the reflection from the open-ended transmission line, agree very well.

In the above examples, we have shown only the calculated input impedance data. The computer output also includes the current distribution and the radiation pattern of the antennas investigated, but it would be impossible to show all of this information in this report. Figure 9 illustrates the calculation of a radiation pattern of a ten-element Yagi antenna array previously calculated by King.[7] The radiation pattern calculated using the present program is seen to agree well with King's calculated pattern.

With the wire antenna program we can treat with surprisingly good results some configurations that one does not at first associate with linear antennas.

Figure 10 shows an example of a structure composed of cylinders, tapered cylinders and cones, that has more than a passing resemblance to an aircraft with a tail-cap antenna. In this example, all of the members -- including the air-foil surfaces -- have circular cross sections, and all except the vertical stabilizer with the tail-cap are co-planar. The dimensions of the members are chosen so that the structure should be an approximate electrical representation of the RB-66 aircraft. A much better representation could have been obtained by using two or more parallel cylinders to represent the flattened air-foil surfaces, dropping the nacelles below the wings and supporting them on struts as they are in the actual aircraft and other refinements. Such refinements would increase both the time required to prepare the data for the computer and the computer time required to obtain the desired solutions. If one were in earnest about the problem, however, such time would be well spent. Again, one could obtain as much accuracy as desired at the cost of increased computer time resulting from the increased complexity of the structure analyzed.

In spite of the comparative crudity of the representation shown in Fig. 10, however, surprisingly useful and accurate results are obtained. (The inaccuracy, it should be pointed out, is not in the answers provided by the computer for the structure analyzed, but in the representation of the actual aircraft by that structure.) The computer calculation predicts the resonant peak in radiation resistance associated

$\frac{1}{16}$ " WIRE

90°

15"
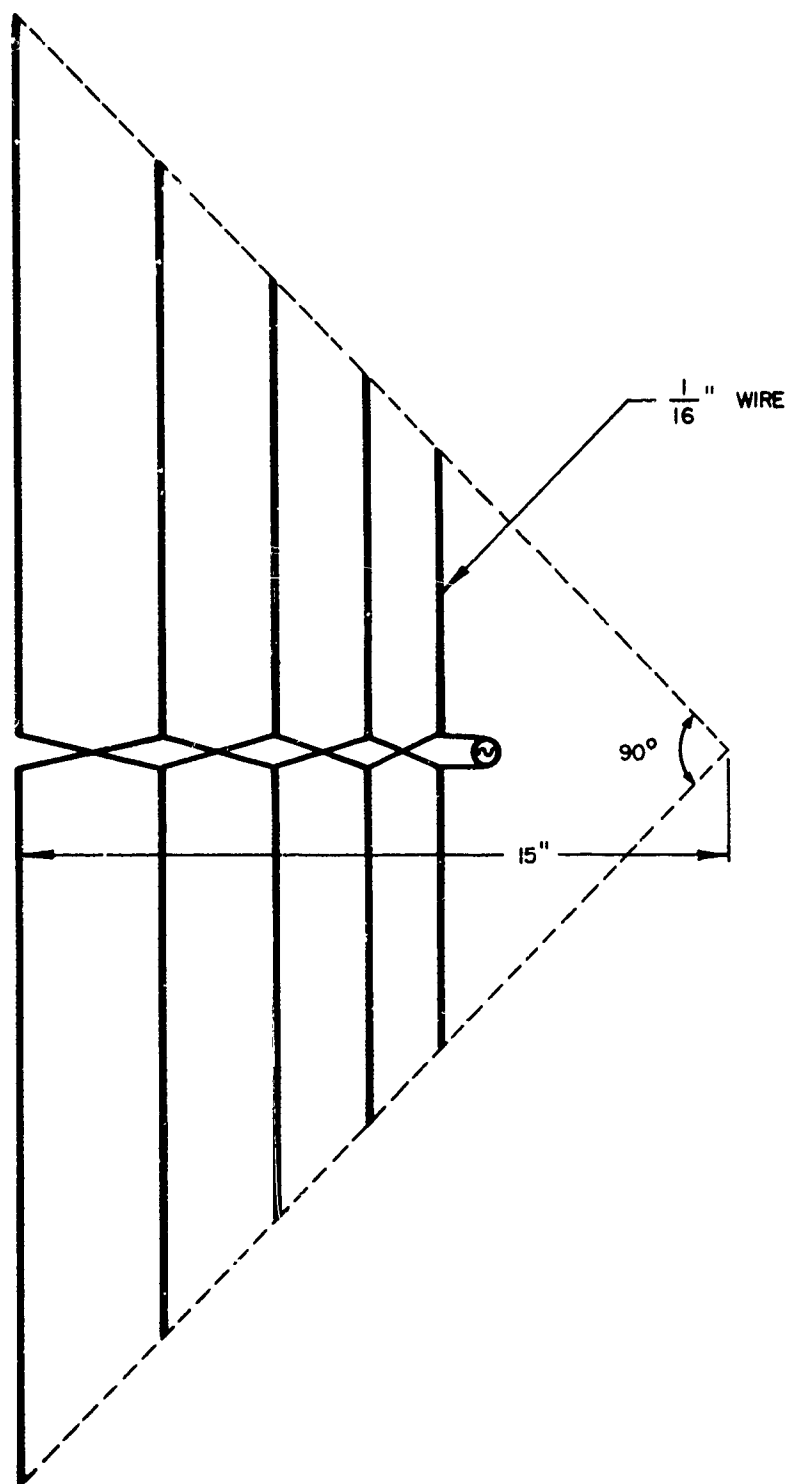
Fig. 6   Log-Periodic Array of Five Elements Fed from
          200 ohm Transmission Line

Fig. 7   Input Impedance of Log-Periodic Array of Five
          Elements from 170 MHz to 270 MHz in Steps of 10 MHz
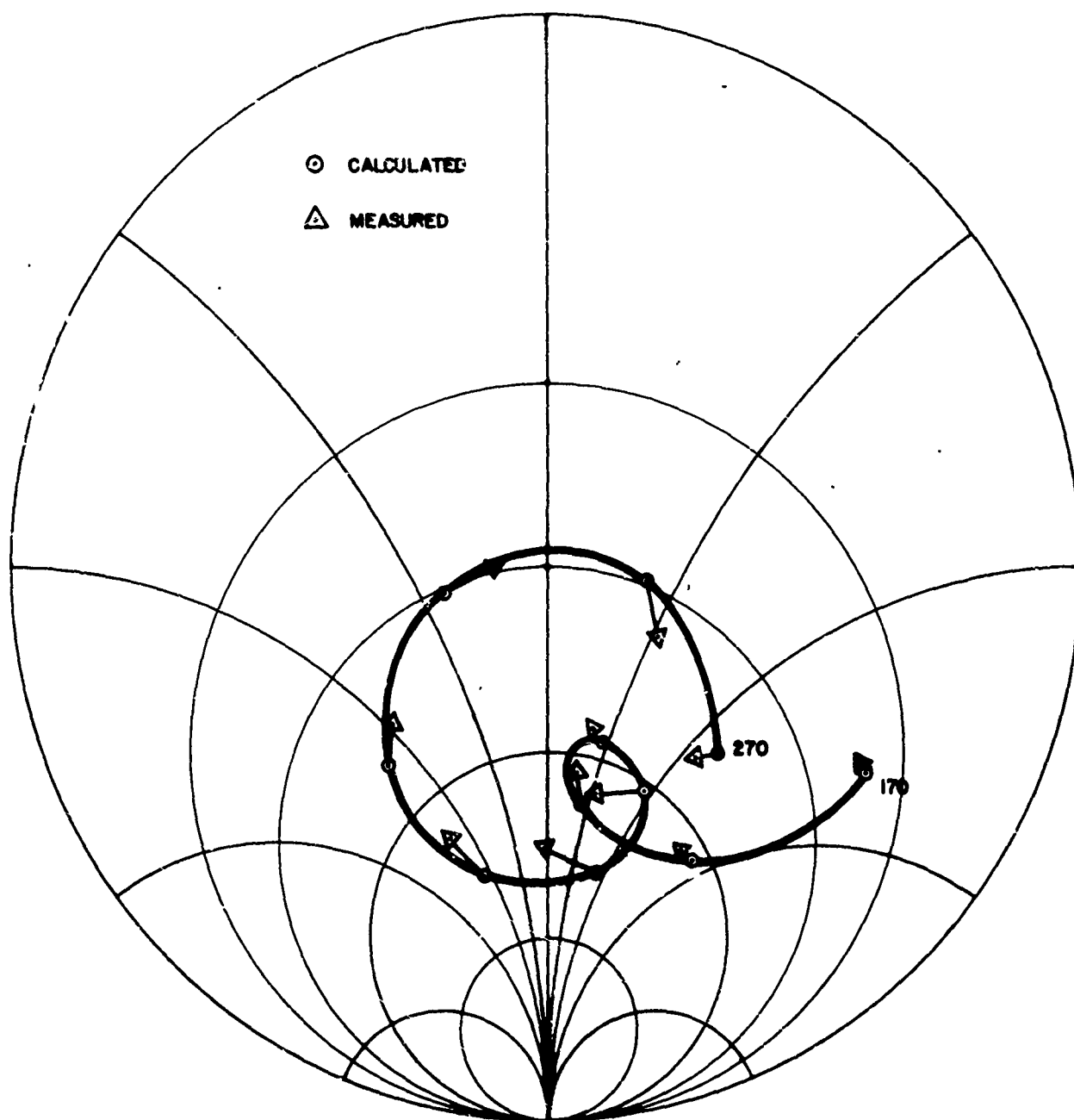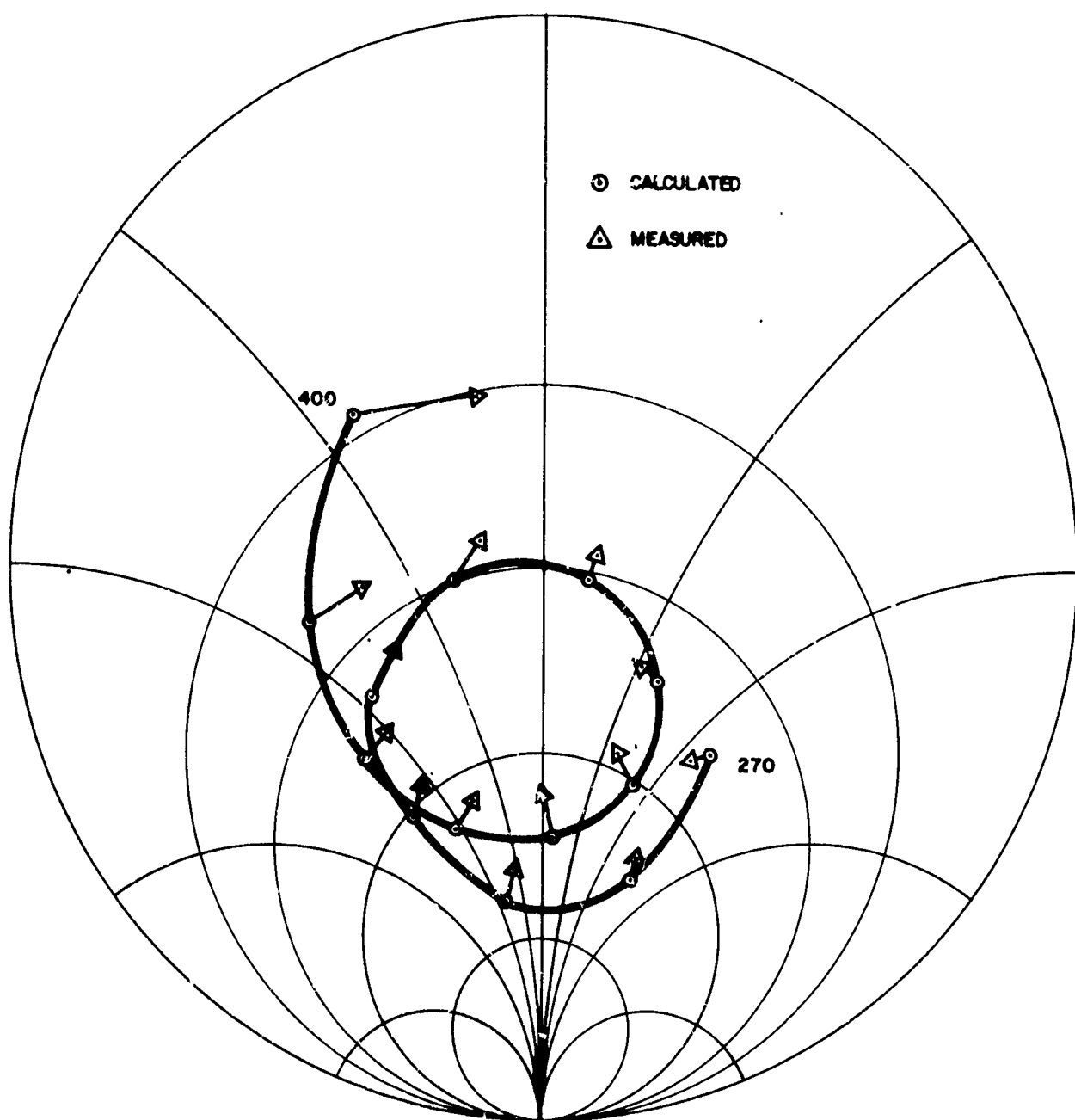   (Chart Impedance = 50 ohms)

26

Fig. 8   Input Impedance of Log-Periodic Array of Five
          Elements from 270 MHz to 400 MHz in Steps of 10 MHz
          (Chart Impedance ≈ 50 ohms)

27

R. King

Andreasen - Tanner

$\phi = 0$
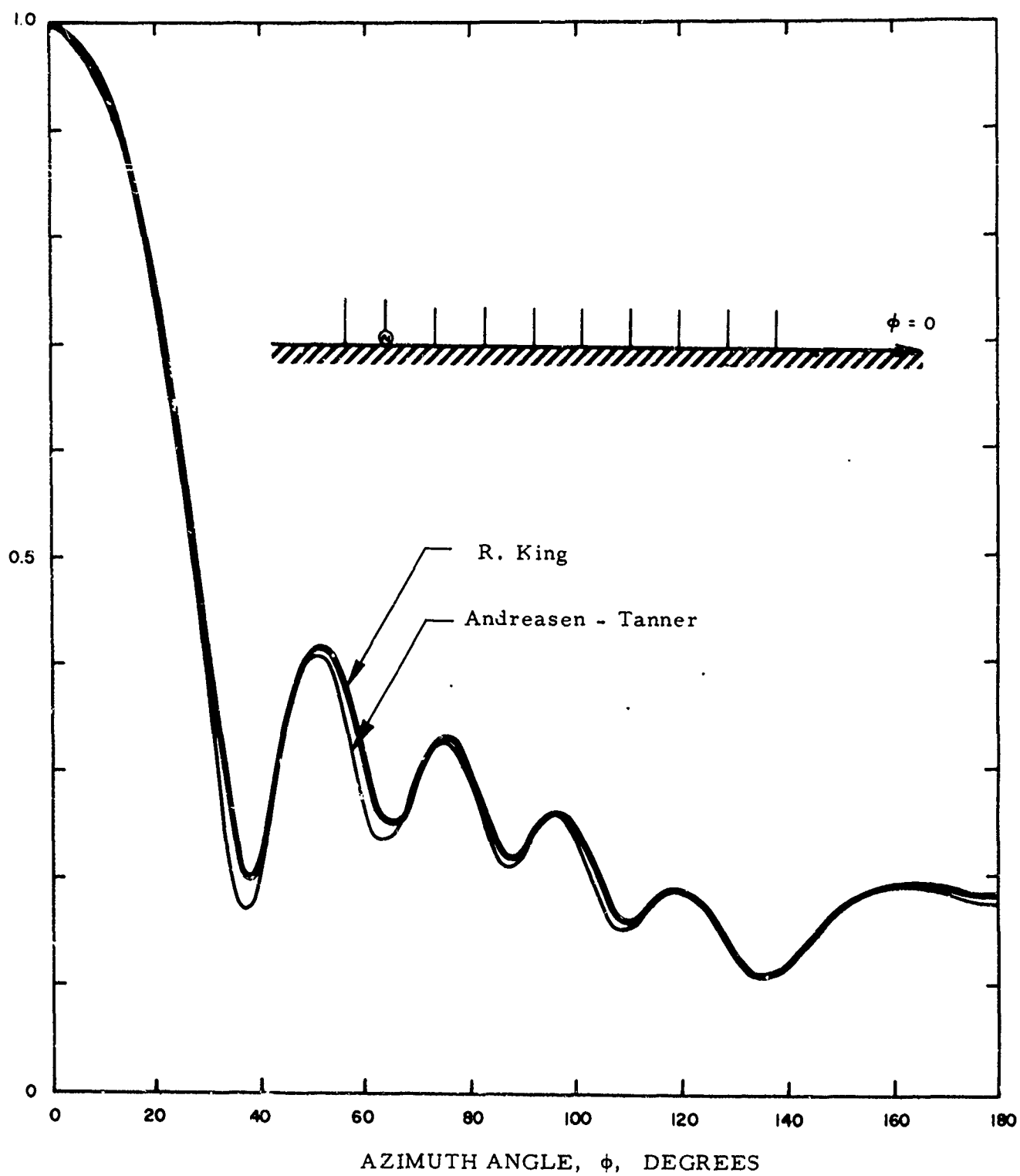
AZIMUTH ANGLE, ϕ, DEGREES

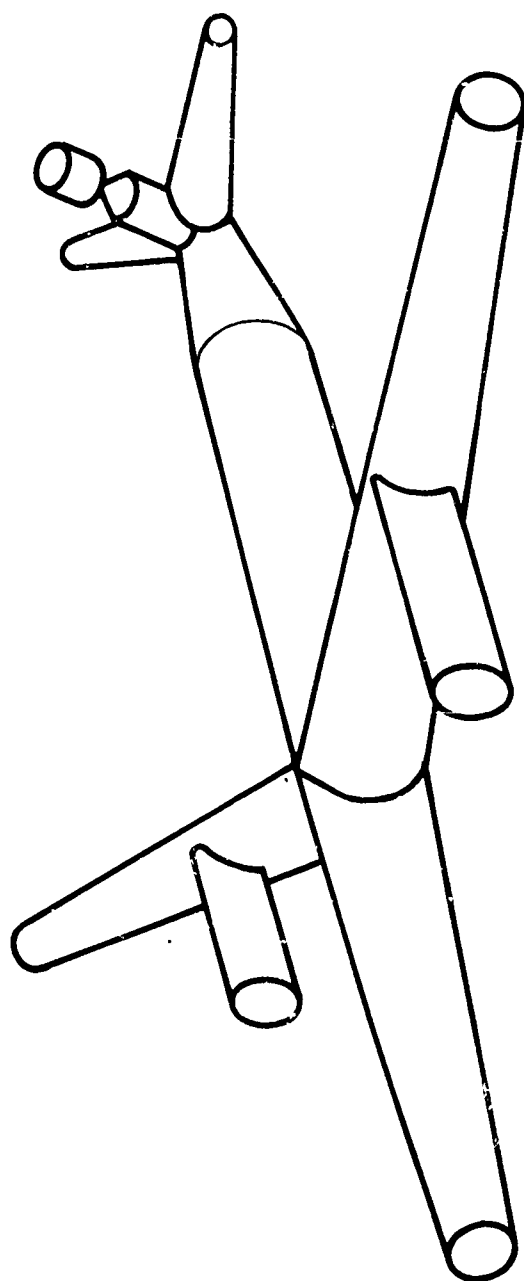Fig. 9   Radiation Pattern of Ten Element Yagi-Array

Fig. 10   Crude Model of RB-66 Aircraft with Tail-Cap Antenna

29

with airframe resonance as well as other aspects of the impedance be-
havior. When suitable corrections are made to allow for the rather
substantial disparity between the actual feed gap region and that in-
corporated in the representation, the calculated impedances -- both
resistance and reactance -- agree with the impedances measured
experimentally on a model of the actual aircraft within approximately
twenty percent at those points checked.

The computer calculation provides rather interesting data on
the distribution of currents on the airframe members. These currents,
for a frequency near airframe resonance, are shown in Fig. 11. In
the figure, the airframe members are represented by the lines forming
the axes of the members and the currents are plotted vertically --
picket-fence fashion -- along these lines. The phases of the currents
vary little, only a few degrees from one end of any member to the
other, and are indicated by the phases shown on the diagram, which
apply to the currents at the center of each linear member composing
the airframe. The finite values of current at the extremities of the
members show the amount of current flowing onto the flat end-caps of
the cylindrical members.

Another good measure of the accuracy of the results provided
by the calculation is in the correspondence of the measured with the
calculated radiation patterns. This comparison is shown in Fig. 12
for a frequency somewhat higher than the airframe resonance fre-
quency (the experimental measurements were made a number of years
ago and only limited data were available). It is evident that the com-
puter has predicted all of the major features of the patterns. The only
significant discrepancy is in the null below the aircraft in the longi-
tudinal principal plane pattern (top center) where the computer predicts
a significantly deeper null than was measured. The two small vestigial
pattern lobes -- the one directed up and forward, and the other rear and
down on this pattern -- are predicted. Since the patterns are changing
quite rapidly with frequency, the discrepancy in the downward null may
well be due to a relatively minor misjudgment in the choice of dimen-
sions for the linear element representation of the aircraft. It is almost
certain that a more elaborate representation would overcome what dis-
crepancies do exist.

Calculations were also made to verify measurements made on a
center-fed whip antenna described elsewhere.[15,16] Calculated and
measured values of the input impedance are shown in Table 2. The
agreement between calculations and measurements is only fair. The
discrepancy between the calculated and the measured impedance values
is ascribed to differences in the experimental and the theoretical models
used for the antenna.

30

Φ = PHASE OF CURRENT
RELATIVE TO GAP
VOLTAGE

ON VERTICAL STABILIZER
Φ = 70°

Φ = 135°

Φ = -23°

Φ = -1.5°

Φ = -8°

Φ = -4°

Φ = -147°
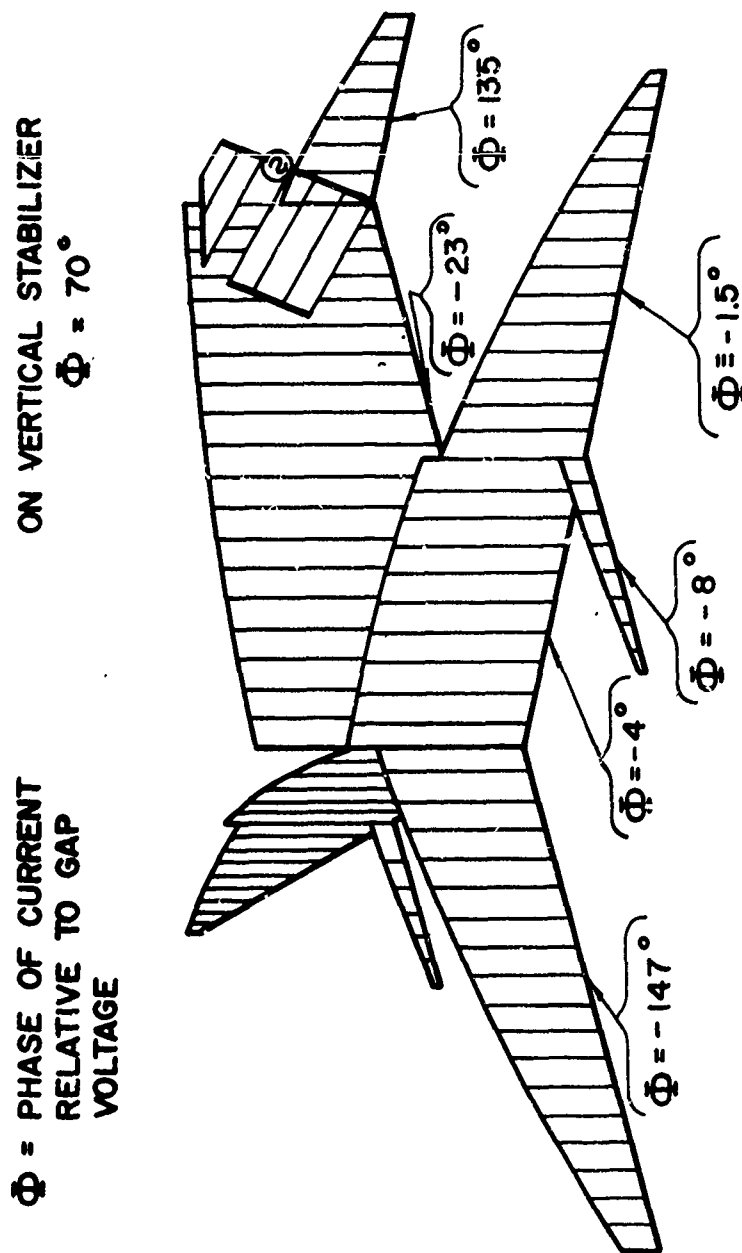
FIG. II CURRENT DISTRIBUTION ON AIRCRAFT WITH TAIL-CAP ANTENNA AT AIRFRAME RESONANCE
FREQUENCY

31
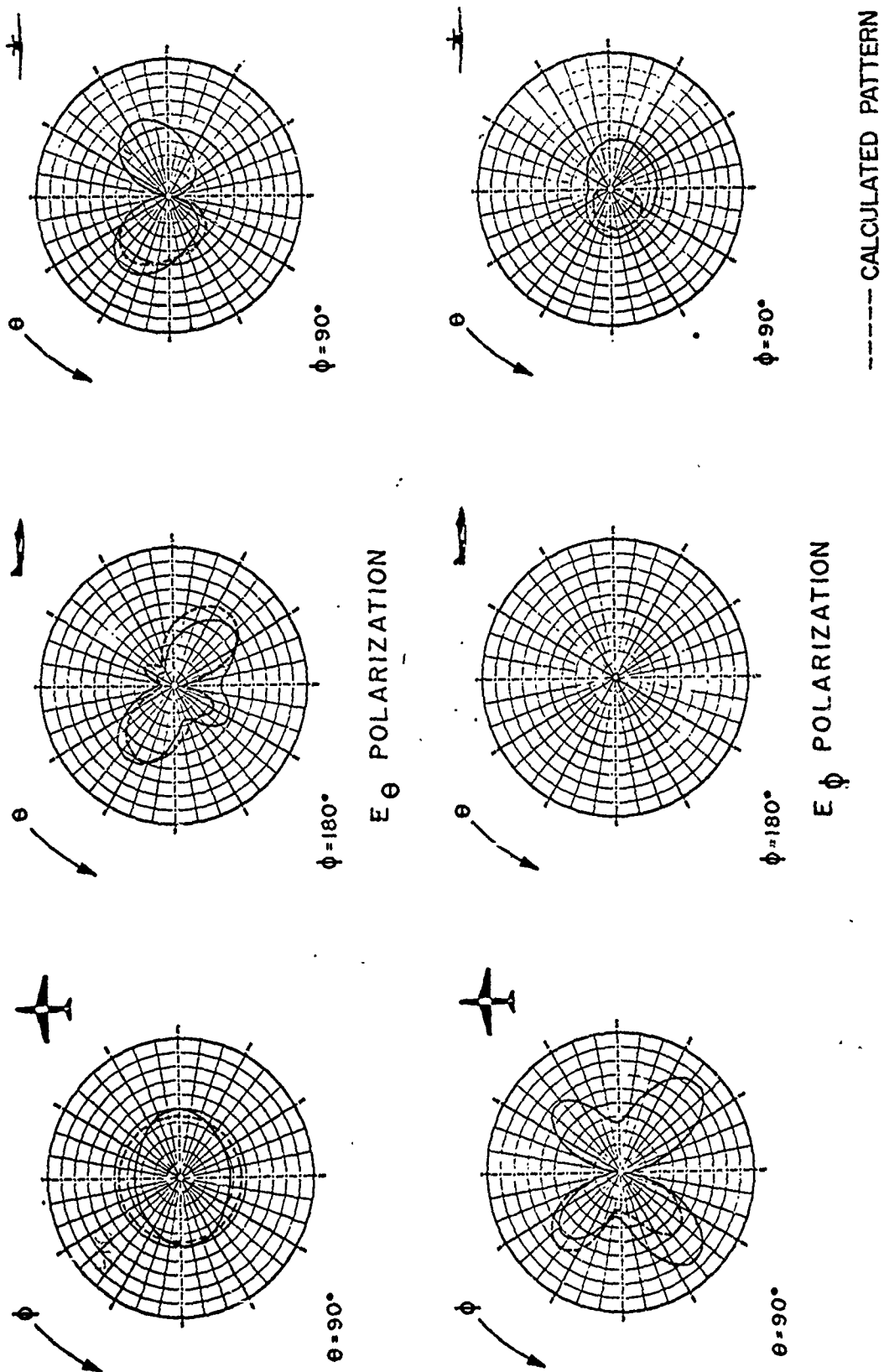
Fig. 12 COMPARISON OF CALCULATED AND MEASURED PATTERNS
RB-66 AIRCRAFT WITH TAILCAP ANTENNA

----- CALCULATED PATTERN

E_θ POLARIZATION

E_ϕ POLARIZATION

$\phi = 90°$

$\phi = 180°$

$\theta = 90°$

Table 2

Calculated and Measured Input Impedance

of Center-Fed Whip Antenna

Band	Frequency MHz	Calculated Input Impedance		Measured Input Impedance	
		R Ω	X Ω	R Ω	X Ω
I	30 33	80 108	- 74 56	30 72	- 82 35
II	33	84	- 84	41	-106
IV	47.5	150	138	185	30
V	47.5 53	72 156	- 90 193	60 205	-175 - 55
VI	53	105	74	70	- 85
IX	70.5	293	528	600	400
X	70.5 76	218 437	435 752	450 700	250 -200

Finally, calculations were made on the compact VHF antenna shown in Fig. 13. The principal results of the calculations at 30 MHz are summarized in Table 3. It is interesting to notice that the input impedance of the antenna drops as the antenna is raised above the ground plane. This behavior is also expected from the theory of coupled antennas. From average-gain calculations it is concluded that the results for the input resistance are within 20 percent of the true values. The small electrical size of the antenna puts a serious strain on the accuracy of the program, the accuracy deteriorating as the electrical size of the antenna approaches zero. The reason for the deteriorating accuracy for electrically small antennas is that the constant-current term and the cosine-current term used in the expansion of the current distribution within each integration interval become degenerate for zero length of the interval. This quasi-degeneracy for electrically small antennas can be removed by using a different representation for the current distribution. The program was applied unsuccessfully to a compact HF antenna with an overall size of 0.01 wavelengths; the round-off errors due to the quasi-degeneracy of the constant- and the cosine-current terms were found to be too large.
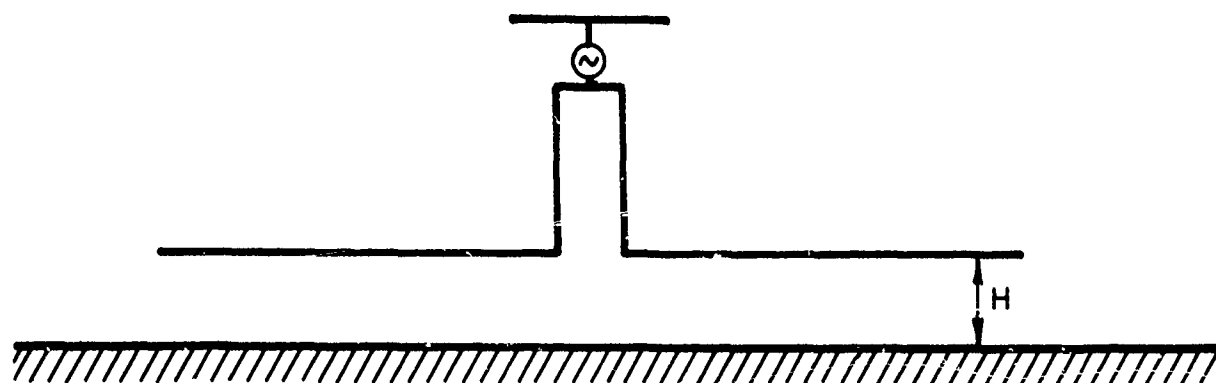
Wire diameter 0.5 inch
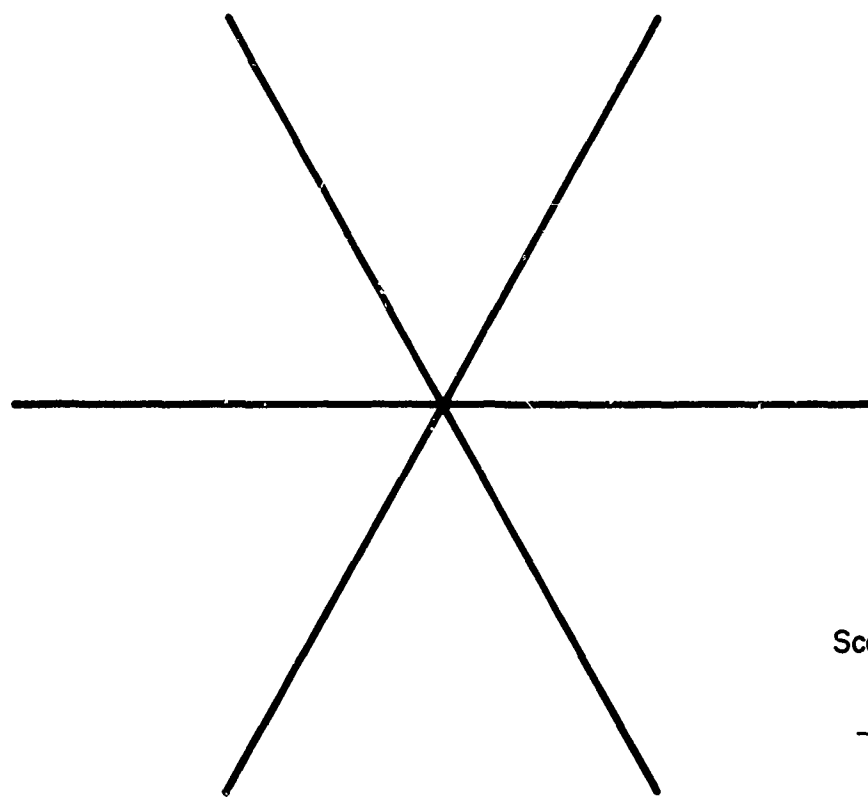
Scale 1:10

1 inch

Fig. 13   Compact VHF-Antenna

35

Table 3

Calculated Data for Compact VHF-Antenna at 30 MHz

Height H Above Ground Plane Inches	Input Resistance, Ohms	Input Reactance, Ohms	Maximum Gain* dB	Gain* at Elevation 30° dB	Gain* at Elevation 60° dB
0	0.87	- 571	5.30	4.04	- 0.77
36	0.61	- 938	6.00	4.16	- 1.87
120	0.42	- 938	7.61	0.50	-11.4

*Gain is referenced to an isotropic radiator.

8. CONCLUSION

The computer program developed will evaluate the properties of virtually any wire antenna. The results shown here have served only to illustrate the applicability of the program. Besides the advantages of speed, economy, and flexibility relative to experimental methods, the numerical approach provides answers with a precision and a wealth of detail completely beyond the reach of experimental techniques in most cases. This detail and precision can provide the basis for enhanced insight into the operation of the antennas analyzed, leading in most cases to more efficient, more economical, and higher performance designs.

REFERENCES

1. H. Hertz, "Untersuchungen Ueber Die Ausbreitung Der Elektrischen Kraft," Wied. Ann, 36, 1, (1888).

2. L. Brillouin, "Sur L'origine de la Résistance de Rayonnement," Radioélectricité 3, pp. 147-152, (1922).

3. E. Hallén, "Theoretical Investigations into the Transmitting and Receiving Qualities of Antennas," Nova Acta Royal Soc. Sci. Ups. (1938).

4. S. A. Schelkunoff, "Theory of Antennas of Arbitrary Size and Shape," IRE Proc., 29, pp. 493-521, (Sept. 1941).

5. S. A. Schelkunoff, "Advanced Antenna Theory," John Wiley and Sons, Inc., New York, (1952).

6. C. T. Tai, "A New Interpretation of the Integral Equation Formulation of Cylindrical Antennas," IRE Trans. PGAP-3, pp. 125 - 127, (July 1955).

7. R. W. King, "The Linear Antenna - Eighty Years of Progress," Proc. IEEE, Vol. 55, No. 1, pp. 2 - 16 (January 1967).

8. K. K. Mei, "On the Integral Equations of Thin Wire Antennas," IEEE Trans. PGAP-13, pp. 374-378, (May 1965).

9. A. Baghdasarian and D. J. Angelakos, "Scattering from Conducting Loops and Solution of Circular Loop Antennas by Numerical Methods, " Proc. IEEE, Vol. 53, No. 8, pp. 818 - 822, (August 1965).

10. J. H. Richmond, "Computer Solutions of Scattering Problems," Proc. IEEE, Vol. 53, No. 8, pp. 796 - 804 (August 1965).

11. R. F. Harrington, "Matrix Methods for Field Problems," Proc. IEEE, Vol. 55, No. 2, pp. 136 - 149 (February 1967).

12. S. Silver, "Microwave Antenna Theory and Design," Vol. 12, MIT Radiation Lab Series, McGraw-Hill Book Company, Inc. New York, (1949).

13. R. W. King, "The Theory of Linear Antennas," Harvard University Press, Cambridge, Mass. (1956).

REFERENCES (continued)

14. J. A. Stratton, "Electromagnetic Theory," McGraw-Hill Book Company, New York (1941).

15. AVCO Corporation, "Development of an Improved Center-Fed Whip Antenna," Final Report No. 4, Contract DA 36-039 SC-90897 (3 November 1963).

16. W. P. Czerwinski, "On a Foreshortened Center-Fed Whip Antenna," IEEE Trans. Vol. VC-15, No. 2, pp. 33-40, (October 1966).

Acknowledgment

APPENDIX A

Dipole Radiation Fields

The reduced integral equations for the wire antenna, Eq. (11), is given in terms of vector functions $\overline{G}_O$, $\overline{G}_c$, and $\overline{G}_s$ that represent the electric field radiated by a dipole carrying a constant, a cosinoidal, or a sinusoidal current respectively. These vector functions will be derived here.

Calculation of $\overline{G}_{c \atop s}(\overline{R}_o, \hat{z}, \Delta)$

Consider the dipole shown in Fig. A-1 of length Δ and oriented in the direction $\hat{z}$. We want to calculate the electric field that this dipole radiates in a point with radius vector $\overline{R}_O$ using the center of the dipole as the origin, when the current distribution on the dipole is of the form:

$$I(z) = {\cos \atop \sin}(kz) \qquad\qquad (A\text{-}1)$$

where k is the free space propagation constant. This problem was solved almost a half century ago by Brillouin.[2] His results can be found in a convenient form in the textbook by Stratton.[14] Thus, for the dipole considered here, we find the following exact expressions for the z- and the ρ-components of the electric field

$$\frac{1}{k}\hat{z}\cdot\overline{G}_{c \atop s}(\overline{R}_o, \hat{z}, \Delta) = j30\left[\frac{e^{-jkR_2}}{kR_2}\ {-\sin \atop \cos}\left(\frac{k\Delta}{2}\right) - \frac{e^{-jkR_1}}{kR_1}\ {\sin \atop \cos}\left(\frac{k\Delta}{2}\right)\right.$$

$$-\left(\frac{1}{kR_2}+j\right)\frac{kz-\dfrac{k\Delta}{2}}{kR_2}\ \frac{e^{-jkR_2}}{kR_2}\ {\cos \atop \sin}\left(\frac{k\Delta}{2}\right)$$

$$\left.+\left(\frac{1}{kR_1}+j\right)\frac{kz+\dfrac{k\Delta}{2}}{kR_1}\ \frac{e^{-jkR_1}}{kR_1}\ {\cos \atop -\sin}\left(\frac{k\Delta}{2}\right)\right] \qquad (A\text{-}2)$$

and

$$\frac{1}{k} \hat{\rho} \cdot \overline{G}_{C_S} (\overline{R}_o, \hat{z}, \Delta) = \frac{-j30}{k\rho} \left\{ \left\langle kz - \frac{k\Delta}{2} \right\rangle \frac{e^{-jkR_2}}{kR_2} \left\{ \frac{-\sin}{\cos} \right\} \frac{k\Delta}{2} \right.$$

$$- \left\langle kz + \frac{k\Delta}{2} \right\rangle \frac{e^{-jkR_1}}{kR_1} \left\{ \frac{\sin}{\cos} \right\} \frac{k\Delta}{2} + \frac{e^{-jkR_2}}{kR_2} \left[-\frac{1}{kR_2} + j \frac{\left\langle kz - \frac{k\Delta}{2} \right\rangle^2}{kR_2} \right] \left\{ \frac{\cos}{\sin} \right\} \frac{k\Delta}{2}$$

$$- \frac{e^{-jkR_1}}{kR_1} \left[-\frac{1}{kR_1} + j \frac{\left\langle kz + \frac{k\Delta}{2} \right\rangle^2}{kR_1} \right] \left\{ \frac{\cos}{-\sin} \right\} \frac{k\Delta}{2} \right\} . \qquad \text{(A-3)}$$

The distances R_1 and R_2 in these expressions are shown in Fig. A-1. z and ρ are the local coordinates of the observation point

$$z = \hat{z} \cdot \overline{R}_o$$

$$\rho = \hat{\rho} \cdot \overline{R}_o. \qquad \text{(A-4)}$$

Calculation of $\overline{G}_o(\overline{R}_o, \hat{z}, \Delta)$

Assume now that the dipole in Fig. A-1 carries a constant current of strength unity. It is then most convenient to start out with the following exact integral representations for the radiated electric field components

$$\frac{1}{k} \hat{\rho} \cdot \overline{G}_o = j\, 30 \int_{-\frac{k\Delta}{2}}^{\frac{k\Delta}{2}} \frac{\partial^2 \psi}{\partial(kz)\,\partial(k\rho)}\, d(kt) \qquad \text{(A-5)}$$

and

$$\frac{1}{k} \hat{z} \cdot \overline{G}_o = -j\, 30 \int_{-\frac{k\Delta}{2}}^{\frac{k\Delta}{2}} \left[\frac{\partial^2 \psi}{\partial(kt)^2} + \psi \right] d(kt) \qquad \text{(A-6)}$$

A-2
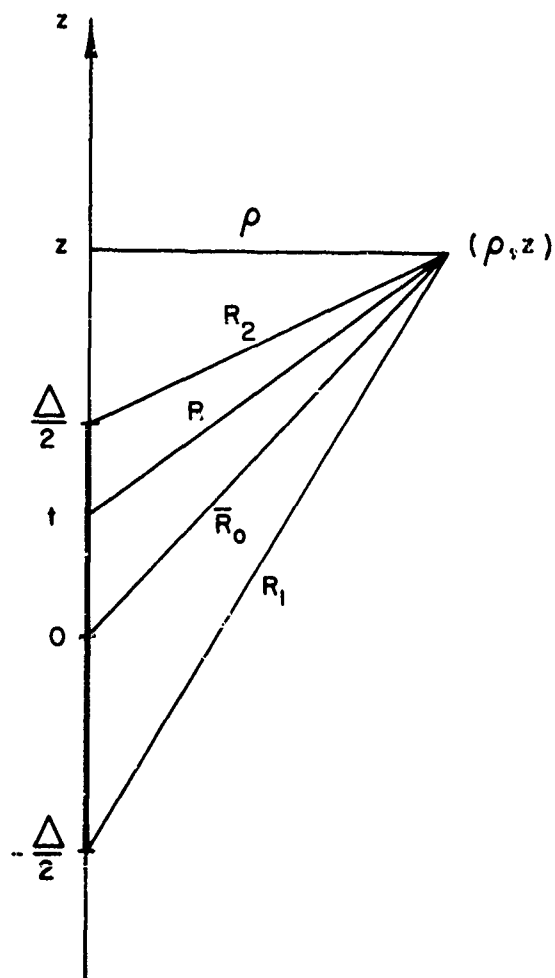
Fig. A-1   Coordinates used in Evaluating the Dipole Radiation Field

where integrations are extended over the length of the dipole. ψ is the spherical wave function

$$\psi = \frac{e^{-jkR}}{kR} .$$
(A-7)

The validity of these expressions can be verified very easily. Let us evaluate first the ρ-component of the field. Introducing

$$\frac{\partial}{\partial z} = - \frac{\partial}{\partial t}$$
(A-8)

$$\frac{\partial R}{\partial \rho} = \frac{\rho}{R}$$
(A-9)

$$\frac{\partial \psi}{\partial (kR)} = - \left(\frac{1}{kR} + j \right) \frac{e^{-jkR}}{kR} .$$
(A-10)

In eq. (A-5), we find

$$\frac{1}{k} \hat{\rho} \cdot \overline{G}_o = - j30 \left[\frac{k\rho}{kR_2} \left(\frac{1}{kR_2} + j \right) \frac{e^{-jkR_2}}{kR_2} - \frac{k\rho}{kR_1} \left(\frac{1}{kR_1} + j \right) \frac{e^{-jkR_1}}{kR_1} \right]. \quad \text{(A-11)}$$

For the z-component of $\overline{G}_o$ we find from Eq. (A-6)

$$\frac{1}{k} \hat{z} \cdot \overline{G}_o = - j30 \left[\frac{\partial \psi}{\partial (kt)} \left[\frac{\frac{k\Delta}{2}}{\underset{-\frac{k\Delta}{2}}{}} + \int_{-\frac{k\Delta}{2}}^{\frac{k\Delta}{2}} \psi \, d(kt) \right] \right]$$

$$= j30 \left[\frac{\frac{k\Delta}{2} - kz}{kR_2} \left(\frac{1}{kR_2} + j \right) \frac{e^{-jkR_2}}{kR_2} + \frac{\frac{k\Delta}{2} + kz}{kR_1} \left(\frac{1}{kR_1} + j \right) \frac{e^{-jkR_1}}{kR_1} - \int_{-\frac{k\Delta}{2}}^{\frac{k\Delta}{2}} \psi \, d(kt) \right] .$$
(A-12)

A-4

The integral over ψ in this equation cannot be evaluated exactly in closed form. However, a reasonably accurate expression valid for small values of $k\rho$ can be obtained as follows. Let us divide the integration path from

$-\dfrac{k\Delta}{2}$ to $\dfrac{k\Delta}{2}$ into one path from $-\dfrac{k\Delta}{2}$ to kz and another path from kz to $\dfrac{k\Delta}{2}$. We find then

$$\int_{-\frac{k\Delta}{2}}^{\frac{k\Delta}{2}} \psi \, d(kt) = \int_{-\frac{k\Delta}{2}}^{kz} \psi \, d(kt) + \int_{kz}^{\frac{k\Delta}{2}} \psi \, d(kt)$$

$$\approx \text{Sign}\left(\frac{k\Delta}{2} + kz\right) \int_{k\rho}^{kR_1} \frac{e^{-jkR}}{\sqrt{(kR)^2 - (k\rho)^2}} \, d(kR)$$

$$+ \text{Sign}\left(\frac{k\Delta}{2} - kz\right) \int_{k\rho}^{kR_2} \frac{e^{-jkR}}{\sqrt{(kR)^2 - (k\rho)^2}} \, d(kR) \qquad (A-13)$$

where
$$\text{Sign}(x) = \frac{x}{|x|} \qquad (A-14)$$

and where we have made use of the following relation

$$\frac{dR}{dt} = \frac{t - z}{R} = \pm \frac{\sqrt{R^2 - \rho^2}}{R}. \qquad (A-15)$$

The upper sign here applies for $t > z$; the lower sign for $t < z$.

A-5

Eq. (A-13) can be further reduced by introducing the substitution

$$x = \frac{R}{\rho}$$

whereby we find

$$\int_{-\frac{k\Delta}{2}}^{+\frac{k\Delta}{2}} \psi \, d(\kappa t) = \text{Sign}\left(\frac{k\Delta}{2} + kz\right) F(kR_1) + \text{Sign}\left(\frac{k\Delta}{2} - kz\right) F(kR_2) \qquad (A\text{-}16)$$

where

$$F(kR) = \int_{1}^{\frac{kR}{k\rho}} \frac{e^{-jk\rho x}}{\sqrt{x^2 - 1}} \, dx. \qquad (A\text{-}17)$$

The evaluation of the function F is different depending on whether $\frac{kR}{k\rho}$ is large or not. If $\frac{kR}{k\rho}$ is large, the function F is most easily evaluated by expressing it as follows:

$$F(kR) = -j \frac{\pi}{2} H_o^{(2)}(k\rho) - \int_{kR}^{\infty} \frac{e^{-jkR}}{\sqrt{(kR)^2 - (k\rho)^2}} \, d(kR) \qquad (A\text{-}18)$$

where we have made use of the following integral representation of the Hankel function of the second kind and of order zero:

$$H_o^{(2)}(y) = j \frac{2}{\pi} \int_{1}^{\infty} \frac{e^{-jyx}}{\sqrt{x^2 - 1}} \, dx. \qquad (A\text{-}19)$$

A-6

The integral in Eq. (A-18) can now be evaluated by expansion of the square root in the integrand and integrating term by term. When we neglect all terms of orders higher than 4 in $k\rho$, we find

$$F(kR) = -j\frac{\pi}{2}H_o^{(2)}(k\rho) + Ci(kR) + j\left[\frac{\pi}{2} - Si(kR)\right]$$

$$-\frac{(k\rho)^2}{4}\left[\frac{\cos(kR)}{(kR)^2} - \frac{\sin(kR)}{kR} + Ci(kR)\right]$$

$$-\frac{3}{32}(k\rho)^4\left[\frac{\cos(kR)}{(kR)^4} - \frac{\sin(kR)}{3(kR)^3} - \frac{\cos(kR)}{6(kR)^2} + \frac{\sin(kR)}{6kR} - \frac{1}{6}Ci(kR)\right]$$

$$+j\frac{(k\rho)^2}{4}\left[\frac{\sin(kR)}{(kR)^2} + \frac{\cos(kR)}{kR} - \frac{\pi}{2} + Si(kR)\right]$$

$$+j\frac{3}{32}(k\rho)^4\left[\frac{\sin(kR)}{(kR)^4} + \frac{\cos(kR)}{3(kR)^3} - \frac{\sin(kR)}{6(kR)^2} - \frac{\cos(kR)}{6kR} + \frac{\pi}{12} - \frac{1}{6}Si(kR)\right]$$

$$(A-20)$$

where Ci and Si are the cosine- and sine-integrals.

If $\dfrac{kR}{k\rho}$ is not very large, the integral over ψ in Eq. (A-12) is most easily evaluated numerically; e.g., by Simpson's rule.

A-7

APPENDIX B

The Current Distribution in an Integration Interval

In the reduction of the integral equations for the current distribution on the wire antenna into a set of simultaneous linear equations in sampled values of the current distribution, it was found that the accuracy of the solution depends strongly upon how the current distribution is assumed to vary between the sampling points. The current distribution in the n'th integration interval, as expressed in Eq. (10), was found to yield a very satisfactory accuracy in most cases. The constants T_n, C_n, and S_n can be expressed as a linear combination of a maximum of three sampled values of current, because a constant-cosine-sine curve can be fitted to three points only. To find the constants of this linear combination, assume that the sampled value of current in the n'th sampling point with wire coordinate $t = t_n$ is I_n, and assume current values I_a and I_b in neighboring points $t = t_a$ and $t = t_b$.

If the curve represented by Eq. (10) is to fit the three points t_a, t_n and t_b, the constants T_n, C_n, and S_n must satisfy the following set of three linear equations

$$
\left\{
\begin{array}{ccc}
1 & \cos\left[k\,(t_a - t_n)\right] & \sin\left[k\,(t_a - t_n)\right] \\[2mm]
1 & 1 & 0 \\[2mm]
1 & \cos\left[k\,(t_b - t_n)\right] & \sin\left[k\,(t_b - t_n)\right]
\end{array}
\right\}
\left\{
\begin{array}{c}
T_n \\[2mm] C_n \\[2mm] S_n
\end{array}
\right\}
=
\left\{
\begin{array}{c}
I_a \\[2mm] I_n \\[2mm] I_b
\end{array}
\right\}
\qquad \text{(B-1)}
$$

which has the solution

$$
T_n = \frac{\left\{I_a,\ I_n,\ I_b\right\}}{D_0}
\left\{
\begin{array}{c}
\sin\left[k\,(t_b - t_n)\right] \\[2mm]
\sin\left[k\,(t_a - t_b)\right] \\[2mm]
-\sin\left[k\,(t_a - t_n)\right]
\end{array}
\right\}
\qquad \text{(B-2)}
$$

$$
C_n = \frac{\left\{I_a,\ I_n,\ I_b\right\}}{D_0}
\left\{
\begin{array}{c}
-\sin\left[k\,(t_b - t_n)\right] \\[2mm]
\sin\left[k\,(t_b - t_n)\right] - \sin\left[k\,(t_a - t_n)\right] \\[2mm]
\sin\left[k\,(t_a - t_n)\right]
\end{array}
\right\}
\qquad \text{(B-3)}
$$

$$S_n = \frac{\{I_a, I_n, I_b\}}{D_0} \left\{ \begin{array}{l} \cos\left[k\,(t_b - t_n)\right] - \Big| \\ \cos\left[k\,(t_a - t_n)\right] - \cos\left[k\,(t_b - t_n)\right] \\ \Big| - \cos\left[k\,(t_a - t_n)\right] \end{array} \right\} \quad (B\text{-}4)$$

where $D_0 = \sin\left[k\,(t_b - t_n)\right] - \sin\left[k\,(t_a - t_n)\right] + \sin\left[k\,(t_a - t_b)\right].$ (B-5)

The currents I_a and I_b in the above expressions will, of course, be related linearly to the sampled currents. If the n'th interval considered above is an "internal" interval with at least one integration interval to each side of it, it is most convenient to let "a" be the $(n-1)$'st sampling point and to let "b" be the $(n+1)$'st sampling point, thus choosing $I_a = I_{n-1}$ and $I_b = I_{n+1}$ (see Table B-1). There are a number of cases, however, that require special consideration. These include the case where one end of the n'th interval is open, and the case where the interval considered adjoins an electric or a magnetic symmetry plane. In these cases, we make use of the fact that the current or its derivative is zero at one end of the interval and select values of t_a, t_b, I_a, and I_b as shown in Table B-1. Other special cases listed in Table B-1 include the case where the interval adjoins a junction of several wires, and the case where it adjoins a gap with a source or a sink. In these cases, we assume the current at the end adjoining the junction or the gap to be unknown (I^G in Table B-1), and we solve for this current by satisfying a gap condition as described in Sec. 4.

Different Types of Interval Locations

Type of Interval Location	$t_a - t_n$	$t_b - t_n$	I_a	I_b
Interval internal	$-\dfrac{\Delta_n + \Delta_{n-1}}{2}$	$\dfrac{\Delta_n + \Delta_{n+1}}{2}$	I_{n-1}	I_{n+1}
Interval open or adjoining magnetic plane for $t < t_n$	$-\dfrac{\Delta_n}{2}$	$\dfrac{\Delta_n + \Delta_{n+1}}{2}$	0	I_{n+1}
Interval open or adjoining magnetic plane for $t > t_n$	$-\dfrac{\Delta_n + \Delta_{n-1}}{2}$	$\dfrac{\Delta_n}{2}$	I_{n-1}	0
Interval adjoining electric plane for $t < t_n$	$-\Delta_n$	$\dfrac{\Delta_n + \Delta_{n+1}}{2}$	I_n	I_{n+1}
Interval adjoining electric plane for $t > t_n$	$-\dfrac{\Delta_n + \Delta_{n-1}}{2}$	Δ_n	I_{n-1}	I_n
Interval adjoining gap or junction of several wires for $t < t_n$	$-\dfrac{\Delta_n}{2}$	$\dfrac{\Delta_n + \Delta_{n+1}}{2}$	I^G	I_{n+1}
Interval adjoining gap or junction of several wires for $t > t_n$	$-\dfrac{\Delta_n + \Delta_{n-1}}{2}$	$\dfrac{\Delta_n}{2}$	I_{n-1}	I^G

APPENDIX C

INSTRUCTIONS FOR USE OF TRG PROGRAM

"WIRTNA"

Control Data 3800 Version

This program will solve a very general class of problems in the area of radiation from wire antennas of essentially arbitrary geometry. The program requires as input the coordinates describing the wire structure, and information on sources and sinks located at gaps along the wire antenna, as well as information on non-radiating networks connecting the gaps. The output consists of the current distribution induced on the wire antenna, the antenna input impedance seen from the generator terminals of the antenna, and the absolute gain of the radiation pattern in any number of specified directions.

The program will handle two types of sources: emf's located in discrete points along the wire structure, and dipole sources placed anywhere with respect to the wire structure. The emf-source is most useful in antenna problems, while the dipole source makes possible the solution of problems of scattering from wire structures.

Introduction

The program "WIRTNA" will solve for the current distribution induced on wire structures composed of linear wire sections joined arbitrarily. The wire structure is assumed to be excited by an emf located in any number of gaps on the wire structure, or by dipole current sources placed anywhere with respect to the wire structure. Each linear wire section is defined by the coordinates and by the wire radius at each end, the wire radius being assumed to vary linearly along the wire. The gap regions are assumed to be conical transmission lines, the source or the sink being located at the apex of the cones. The wire radius must be defined as zero where a gap is desired.

Two types of gaps can be defined, see Fig. 1. The gap at one end of wire section 1 connects a conical wire to a ground plane, while the gaps at the junction of wire sections 5 and 6 connect two conical wires. Any number of wires may be joined, and a gap be defined at each wire going to the junction. In fact, junctions of wires are handled most accurately by the program when a short-circuited gap is defined at each wire of the junction. In each gap an emf is defined in series with a generator impedance which can be a series-or parallel-R-L-C circuit, see Fig. 1. The gaps can be connected by any number of four-terminal networks, see Fig. 2. The program could handle any type of linear network but is presently set up to handle only a two-wire transmission line (or single wire if the network is ground-connected as in Fig. 2B).

The gaps are invariably needed in antenna problems. In scattering problems, the source is not an emf placed in the wire structure but rather a distant antenna; e.g., a simple dipole that will produce a plane wave at the wire structure. In order to enable the solution of scattering problems as well as antenna problems, dipole current sources can be

C-2

defined anywhere with respect to the wire structure. Each dipole source is assumed to have a current distribution varying as Cos (kx) along the dipole, x = 0 being in the center of the dipole, and k being the free space propagation constant. For some applications it may even be desirable to use a combination of gap-emf's and dipole current sources.

The order in which the coordinates of the ends of the linear wire sections are read is not arbitrary. The reading of coordinates must start at a junction or an open end of the wire structure and must proceed along a wire until the next junction or open end is met. Figure 1 shows one possible order in which the wire sections of a specific antenna can be arranged. The positive direction of current is assumed to be the direction in which the wire coordinates are read.

In many applications the current distribution on an antenna is known to possess certain symmetry properties equivalent to the existence of electric or magnetic image planes. While the mutual coupling effect between all parts of the antenna must be taken exactly into account, it is not necessary to let the computer solve for the image currents. Since a substantial amount of computer time can be saved by making use of the symmetry properties of the antenna, the program is written so that the antenna can be imaged in the planes $Z = 0$ and $Y = 0$, see Fig.3. The plane $Z = 0$ can be defined only as an electric "ground plane," while the plane $Y = 0$ can be defined as an electric or a magnetic plane.

The symmetrically excited circular ring array is another example of an antenna which possesses symmetry properties that the program will utilize at a considerable saving in computer time. The circular ring array is assumed to have N antennas, the n'th antenna element being constructed by rotation of the first antenna element, the reference element, through an angle $\frac{360}{N}$ (n-1) degrees about the z-axis, see Fig. 4. A ring array of this type can be excited in N linearly independent "azimuthal" modes. The m'th azimuthal mode is characterized by a gap voltage V_n in the n'th antenna element that is related to the gap voltage V_1 in the reference element as follows:

$$V_n = V_1 e^{j \frac{2\pi}{N}(n-1)m}$$

With this excitation of the ring array, the current distribution $I_n(s)$ in the n'th element will be related to the current distribution $I_1(s)$ in the reference element as follows:

$$I_n(s) = I_1(s) e^{j \frac{2\pi}{N}(n-1)m}$$

where s is a coordinate along the wire.

The symmetry properties of a symmetrically excited ring array can also be made use of to great advantage when the excitation of the ring array is arbitrary, because any excitation of the ring array can be represented by a linear combination of the symmetrical modes of the ring array.

Three types of azimuth variations of the ring array can be handled by the program. The exponential variation described above is the most general variation which can be applied to any ring array according to Floquet's theorem. The program will also handle the cosine- or the sine-variations which may often be used with advantage when such variations are known to be existing.

The program "WIRTNA" is actually written for a ring array. This does not complicate the treatment of single antennas which are merely interpreted as ring arrays with one element.

The program will calculate the radiation pattern gain in any number of directions. The direction of observation is described in terms of the elevation angle θ and the azimuth angle ϕ as shown in Fig. 4. Since the far-field is generally elliptically polarized, the gain of the major axis field component, the gain of the minor axis field component, the gain of the vertical field component, and the gain of the horizontal field component are computed in addition to the total gain. The axial

C-4

ratio of the polarization ellipse, the angle between the major axis of the ellipse and the horizon, and the direction of rotation of the field vector are listed in the pattern output. The effect of a finite conductivity of the ground can be taken into account only in radiation pattern calculations.

The program provides for omitting the contributions to the radiation pattern arising from the dipole current sources. The omission of these contributions to the radiation pattern is usually desired in scattering calculations.

The program will read a maximum of 9 "pattern cards," each pattern card defining a mesh of directions of observations at which the pattern gain is to be evaluated.

The program will handle any number of cases. The input data cards for the cases to be analyzed are stacked, and the last case is terminated by an END-card.

Description of Card Input

The input data for the program can be read according to the following sequence of FORTRAN statements:

```
      DIMENSION ITITLE(5)
      COMPLEX  RVOLT, RAMP
110   READ 1, (ITITLE(I), I = 1, 5) IAZIM, ISYMTRY, NCURSOUR
      IF (ITITLE-3HEND) 120, 200, 120
120   READ 2, NELEM, NWIRE, MSTART, MMAX, EPSGR, CONDGR,
      CONDWR
      NWIRNCUR = NWIRE + NCURSOUR
      DO 130 I = 1, NWIRNCUR
130   READ 3, X1(I), Y1(I), Z1(I), RADIUS 1(I), X2(I), Y2(I), Z2(I), RADIUS 2(I)
      DO 190 NFR = 1, NFREQ
      READ 4, FREQ
      READ 5, (INTEVAL(I), I = 1, NWIRE)
      DO 140 I = 1, NPAT
140   READ 6, IPATTYP(I), NELEVA(I), ELEVSTAR(I), ELEVSTEP(I),
                NPHI(I), PHISTAR(I), PHISTEP(I), ICURPAT(I)
      DO 180 IEXC = 1, NEXCITA
      DO 150 J = 1, NGAPEXC
150   READ 7, I, RVOLT(I), YVOLT(I), ISERPAR(I), OHM(I), HENRYM(I),
                FARADP(I)
      DO 160 I = 1, NCURSOUR
160   READ 8, RAMP(I)
      DO 170 I = 1, NETS
170   READ 9, ITYPENET(I)(NETGAP(I, J), J = 1, 4), PAR1(I), PAR2(I),
                PAR3(I), PAR4(I), PAR5(I), PAR6(I)
180   CONTINUE
      READ 10, IEND
190   CONTINUE
      GO TO 110
200   CONTINUE
      END
```

C-6

Format Statements

1. FORMAT (5A8, 2 (A8, 2X) I5).

2. FORMAT (4I5, F10.0, F10.4, F10.0)

3. FORMAT (8F10.4)

4. FORMAT (1X, F9.4)

5. FORMAT (16I5)

6. FORMAT (A8, 2X, 2(I5, 2F10.4), I5)

7. FORMAT (I5, C(F10.4, F10.4) A8, 2X, 3F10.4)

8. FORMAT (1X, C(F9.4, F10.4))

9. FORMAT (A8, 2X, 4I2, 2X, 6F10.2)

10. FORMAT (A3)

While the above sequence of FORTRAN statements is a valid
method of reading the input information, it should also be pointed out that
the program permits a substantial saving in the input data card prepara-
tion when calculations of an antenna are to be made at several frequencies
for the same number of integration intervals, the same patterns, and for
the same excitation modes. In such cases the information on the integra-
tion intervals, the patterns and the excitation modes is read only for the
first frequency. For each following frequency only the frequency card
need be read, and the program will automatically assume that calcula-
tions are to be made for the same number of integration intervals, the
same patterns, and the same excitation modes as at the   previous fre-
quency.

An explanation of the symbols used in the above sequence of FORTRAN
statements follows:

CONDGR   is the conductivity of the ground z ≈ 0 over which the

antenna is placed, measured in mhos per meter.

See also under EPSGR.

CΦNDWR   is the conductivity of the type of wire composing the antenna, measured in mhos per meter. If CΦNDWR is left blank, the wire conductivity is assumed to be infinite.

ELEVSTAR   is the first elevation angle for which pattern calculations are made.

ELEVSTEP   is the difference between the $(n+1)^{st}$ and the n^{s}th elevation angle for which pattern calculations are made.

EPSGR   is the relative dielectric constant of the ground $z = 0$ over which the antenna is placed. if EPSGR $= 0$, the ground is assumed to be perfectly conducting. If EPSGR $= 1$, the antenna is assumed to be placed in free space. Otherwise, the ground is assumed to be perfectly conducting in the calculation of the current distribrtion, but to have the relative dielectric constant EPSGR in the radiation pattern calculations.

FARADP(I)   is the capacitance (C) of the generator impedance, measured in picofarads, in the I^{s}th gap of the reference antenna.

FREQ   is the frequency in MHz. The card from which FREQ is read must have an "F" in the first column.

HENRYM(I)   is the self inductance (L) of the generator impedance, measured in microhenrys, in the I^{s}th gap of the reference antenna.

C-8

IAZIM   is the azimuth variation assumed in the ring array

considered and may be any of the following symbols:

EXPON   if the azimuth variation is exponential

COS   if the azimuth variation is cosinoidal

SIN   if the azimuth variation is sinusoidal

The symbol for IAZIM must be left justified in the

field allowed. If a single antenna is considered, the

field for IAZIM is merely left blank.

ICURPAT   is used to define whether the contributions from the

dipole current sources to the radiation pattern are

to be included or not. ICURPAT can have two values:

$$\text{ICURPAT} = \begin{cases} \text{1} & \text{if the contributions from the dipole} \\ & \text{current sources are to be included} \\ & \text{in the pattern.} \\ \\ \text{0} & \text{if these contributions are to be ex-} \\ & \text{cluded from the pattern.} \end{cases}$$

IEND   = 3HEND.

INTEVAL(I)   is the number of integration intervals used on the I'th

linear wire section of the reference element. The total

number of intervals between one junction or open end

and another junction or open end of the antenna must be

equal to or greater than 3. The number of integration

intervals must be large enough to assure that no inte-

gration interval exceeds about 0.2 wavelengths.

IPATTYP   is used to define various forms of the pattern gain

output.   IPATTYP can be any of the following symbols:

DB   if the pattern gain in dB relative to an
          isotropic antenna is desired.

POWER   if the power gain relative to an isotropic
         antenna is desired.

VOLTAGE if the amplitude gain relative to an iso-
          tropic antenna is desired.

ISERPAR(I)   is used to determine whether the L, C, and R of the

generator impedance in the I'th gap of the reference

antenna are in series or in parallel (see Fig. 1).

ISERPAR can be any of the following symbols:

  SERIES   if a series combination is considered.

  PARALLEL   if a parallel combination is considered.

If the field for ISERPAR is left blank, the generator

impedance is assumed to be 0 independent of the

values read for L, C, and R. The symbol for

ISERPAR must be left justified in the field allowed.

ISYMTRY   is used to define the presence of an image of the refer-

ence antenna element in the XZ-plane. ISYMTRY must

be one of the following symbols:

ELECTRIC   if the imaging assumes the XZ-plane to be
              an electric plane (no tangential electric field).

MAGNETIC   if the imaging assumes the XZ-plane to be a
              magnetic plane (no tangential magnetic field).

If the field allowed for ISYMTRY is left blank, no image

of the reference element is introduced in the XZ-plane.

ITITLE   is read from the first card of each case and serves as

identification for the customer. The information on this

card is also printed on the output listing.

C-10

ITYPENET(I)   is used to define the network type of the I'th four-terminal network connecting the gaps of the antenna. In the present version of the program, ITYPENET can only be the following symbol:

TRLINE   which stands for a two-wire transmission line and must be left justified in the field allowed.

MSTART   is the lowest mode number of the ring array for which calculations are to be made. When a single antenna is considered, choose MSTART = 0.

MMAX   is the highest mode number of the ring array for which calculations are to be made. When a single antenna is considered, choose MMAX = 0.

NCURSOUR   is the number of dipole current sources used.

NELEM   is the number of elements considered in the ring array. When a single antenna is considered, choose NELEM = 1.

NELEVA   is the number of elevation angles for which pattern calculations are made. The gain is computed NPHI times for each value of the elevation angle.

NETGAP(I, J)   is the number of the gap to which the J'th terminal of the I'th four-terminal network is connected. NETGAP can have values from 1 through NGAP, but can also have the value 0, which is used to indicate a ground connection. The ordering of the four terminals of a network is as

C-11

NETGAP(I, J)
continued

shown in Fig. 2. For the example in Fig. 2a, the four values of NETGAP would be 4, 3, 6, and 5. For the example in Fig. 2b, the four values of NETGAP would be 1, 0, 2, and 0.

A 180 degree phase shift (physically obtained by a phase inverter, or by twisting the transmission line) can be introduced by interchanging two of the NETGAP values. An additional 180 degree phase shift introduced in the examples in Fig. 2a and Fig. 2b could be obtained by choosing the following values for NETGAP: 3, 4, 6, and 5 for example 2a; and 1, 0, 0 and 2 for example 2b.

NETS

is the number of four-terminal networks connected to the gaps of the antenna. This number is not an input parameter. The program keeps automatically a count of the number of "network" cards read.

NEXCITA

is the number of "excitation modes" for which calculations are to be made. Each excitation mode corresponds to a particular set of applied emf's and generator impedances in the gaps of the reference element and, if present, a particular set of dipole current sources. For a single antenna with only one gap, NEXCITA would most often be 1. This number is not an input parameter. The program keeps automatically a count of the number of excitation modes.

NFREQ

is the number of frequencies for which the antenna is to be analyzed. This number is not an input parameter. The program keeps automatically a count of the number of frequencies.

C-12

NGAP   is the number of gaps on the reference antenna element.
              This number is determined by the computer, and the
              gaps are numbered from 1 to NGAP in the order in
              which the gaps are encountered when the wire co-
              ordinates are being read. The double gap shown in
              Fig. 1 counts as two gaps.

NGAPEXC   is the number of gaps of the antenna that are not
              short-circuited.

NPAT   is the number of "pattern" cards read. This number is
              not an input parameter. The program keeps automati-
              cally a count of the pattern cards as they are read.

NPHI   is the number of azimuth angles for which pattern cal-
              culations are made. The gain is calculated NELEVA
              times for each value of the azimuth angle.

NWIRE   is the number of linear wire sections composing the
              reference antenna element.

ФHM(I)   is the resistance (R) of the generator impedance,
              measured in ohms, in the I'th gap of the reference
              antenna.

PAR1(I)   is a quantity that describes a certain parameter of
              the I'th network connecting the gaps. For the trans-
              mission-line network, PAR1 is the impedance of the
              transmission line (in ohms).

C-13

PAR2(I) is a quantity that describes a certain parameter of the I'th network connecting the gaps. For the transmission line network, PAR2 is the length of the transmission line (in inches if all other dimensions of the antenna were read in inches – otherwise this length is measured in wavelengths).

PHISTAR is the first azimuth angle for which pattern calculations are made.

PHISTEP is the difference between the (n+1)st and the n'th azimuth angle for which pattern calculations are made.

RADIUS 1(I) is the wire radius at the first end point of the I'th linear wire section of the reference antenna element. RADIUS 1 is measured in inches. RADIUS 1 must be 0 where a gap is located.

RADIUS 2(I) is the wire radius at the second end point of the I'th linear wire section of the reference antenna element. RADIUS 2 is measured in inches. RADIUS 2 must be 0 where a gap is located.

RAMP(I) is the complex current flowing in the center of the I'th dipole current source and is measured in amperes.

RVΦLT(I) is the complex emf applied in the I'th gap of the reference antenna and is measured in volts.

X1(I) is the x-coordinate of the first end point of the I'th linear wire section of the reference antenna element. X1 is measured in inches.

C-14

X2(I)   is the wire radius at the second end point of the I'th
                         linear wire section of the reference antenna element.
                         X2 is measured in inches.

Y1(I)   is the y-coordinate of the first end point of the I'th
                         linear wire section of the reference antenna element.
                         Y1 is measured in inches.

Y2(I)   is the wire radius at the second end point of the I'th
                         linear wire section of the reference antenna element.
                         Y2 is measured in inches.

Z1(I)   is the z-coordinate of the first end point of the I'th
                         linear wire section of the reference antenna element.
                         Z1 is measured in inches.

Z2(I)   is the wire radius at the second end point of the I'th
                         linear wire section of the reference antenna element.
                         Z2 is measured in inches.

Computer Printout

The computer program will calculate the current distribution on
the antenna, as well as the antenna input impedance and the radiation
pattern. The computer first lists the input data. For each frequency and
each excitation mode, the computer then lists the gap sources and the
networks connecting the gaps (if any). For each azimuthal mode of the
ring array, the computer prints the amplitude (in amperes) and the
phase (in degrees) of the current at the center and at the end points of
each integration interval. The input impedance data printed consists of
the input impedance and admittance seen at each gap. The radiation
pattern printout gives information on the absolute gain of the antenna in
the directions specified. In general, the radiation field will be elliptically
polarized, and the computer prints the gain of the vertical field com-
ponent, the gain of the horizontal field component, the gain of the field
component along the major and minor axes of the polarization ellipse,
as well as the total gain. The computer also prints the axial ratio of the
polarization ellipse, the angle between the major axis and the horizontal
plane, and the sense of rotation of the polarization ellipse.

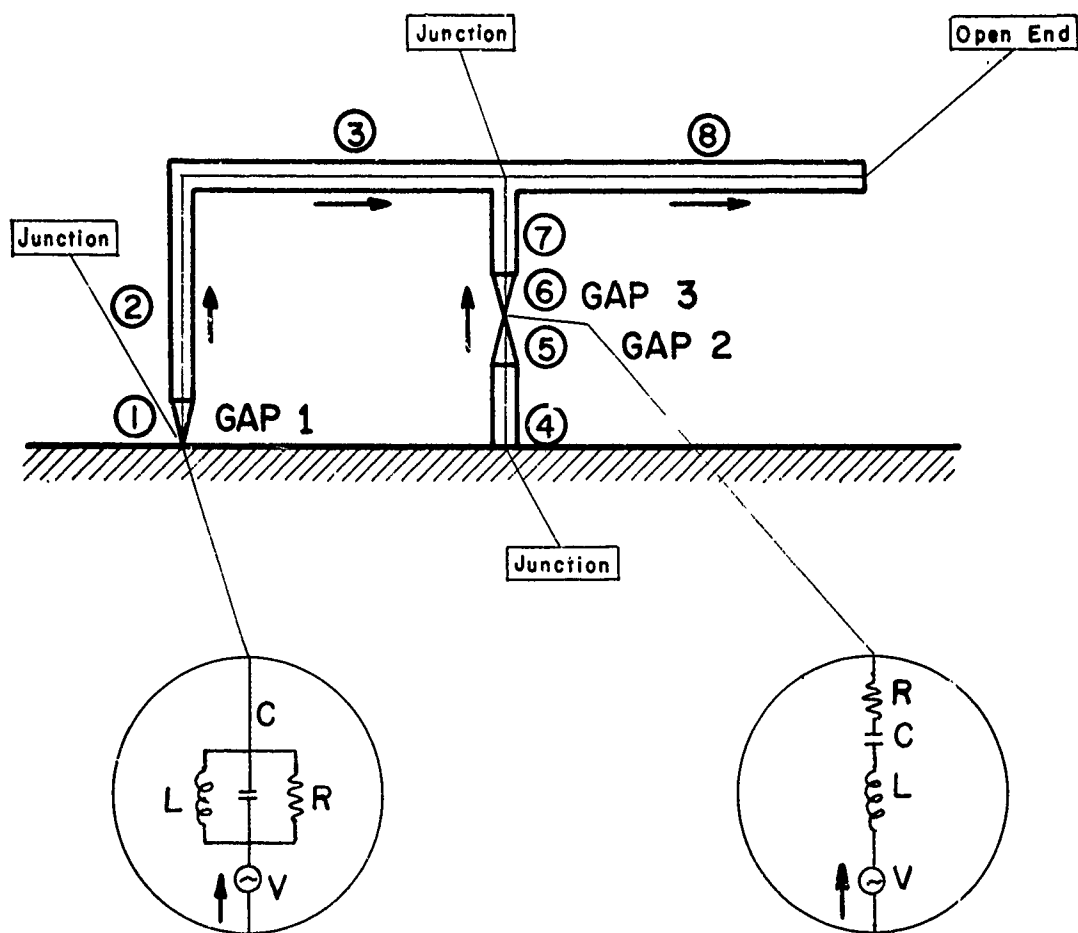The computer finally prints a brief summary of the calculations.
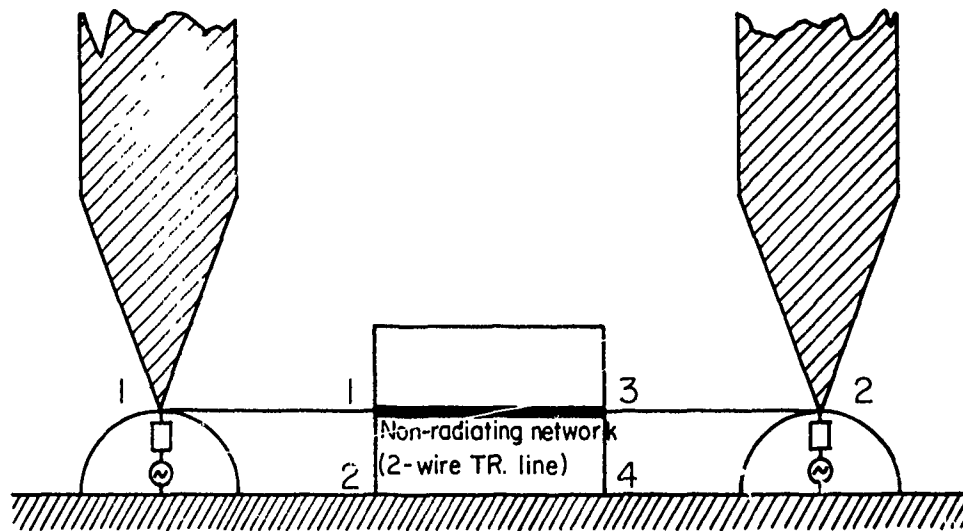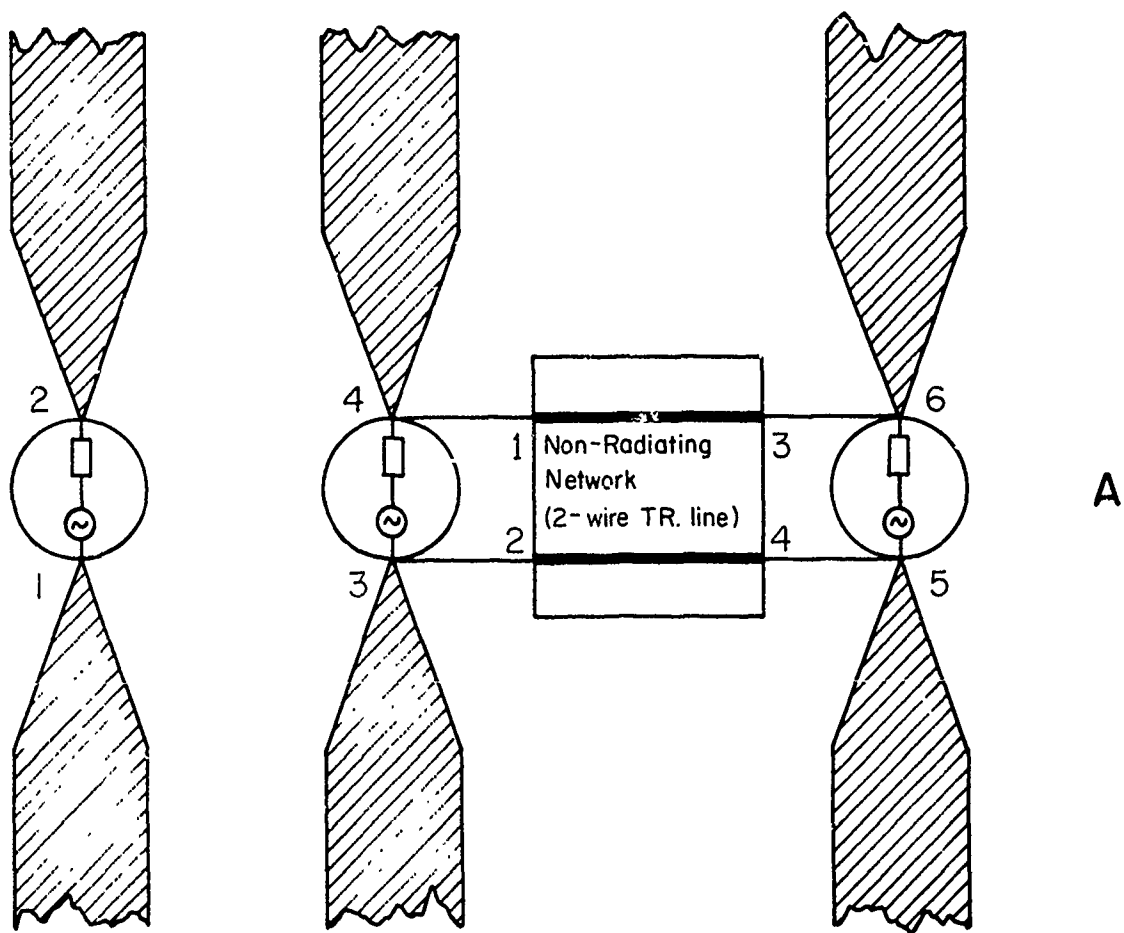
Fig. 1   Wire Antenna Example
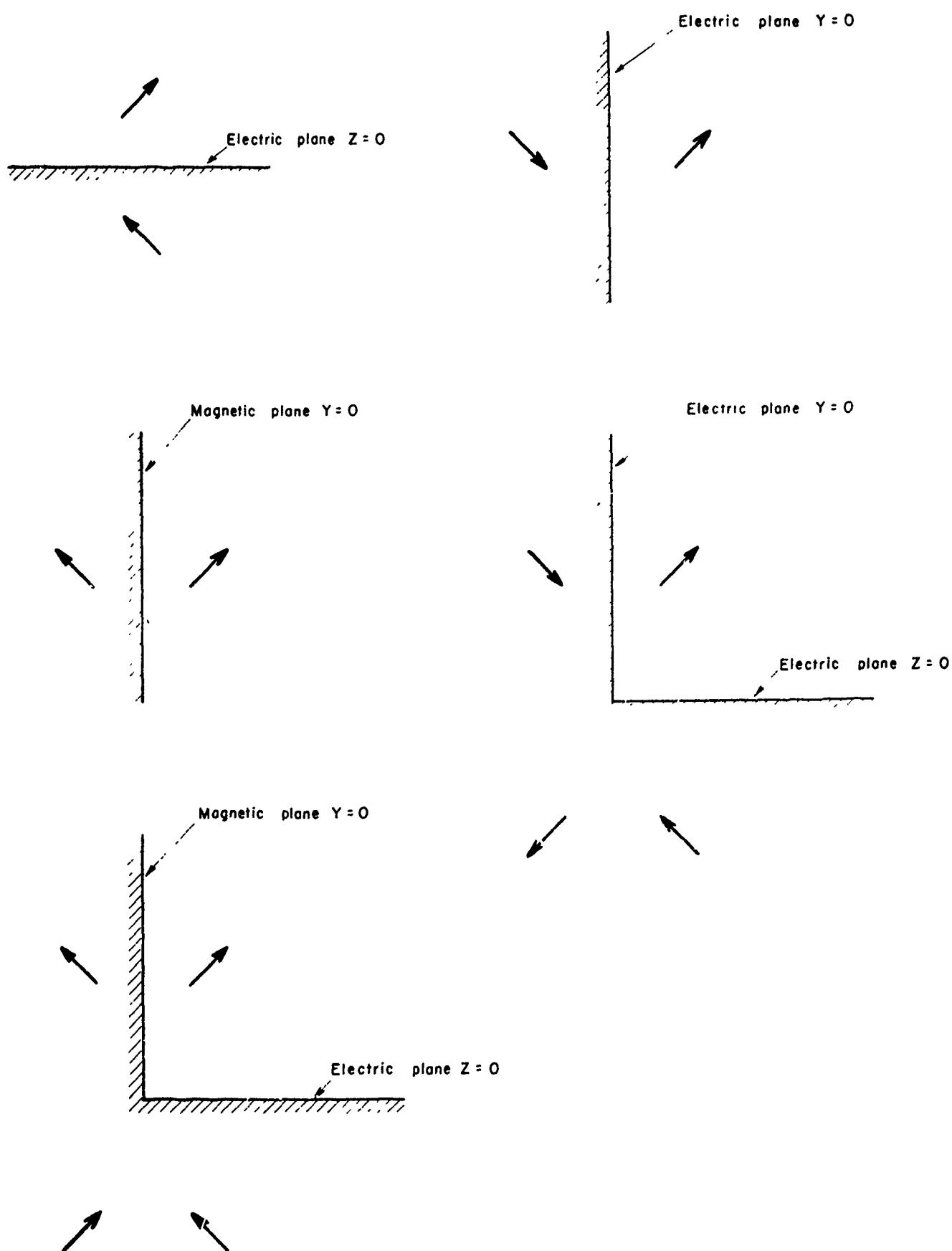
Fig. 2   Connection of Gaps by Non-radiating Networks
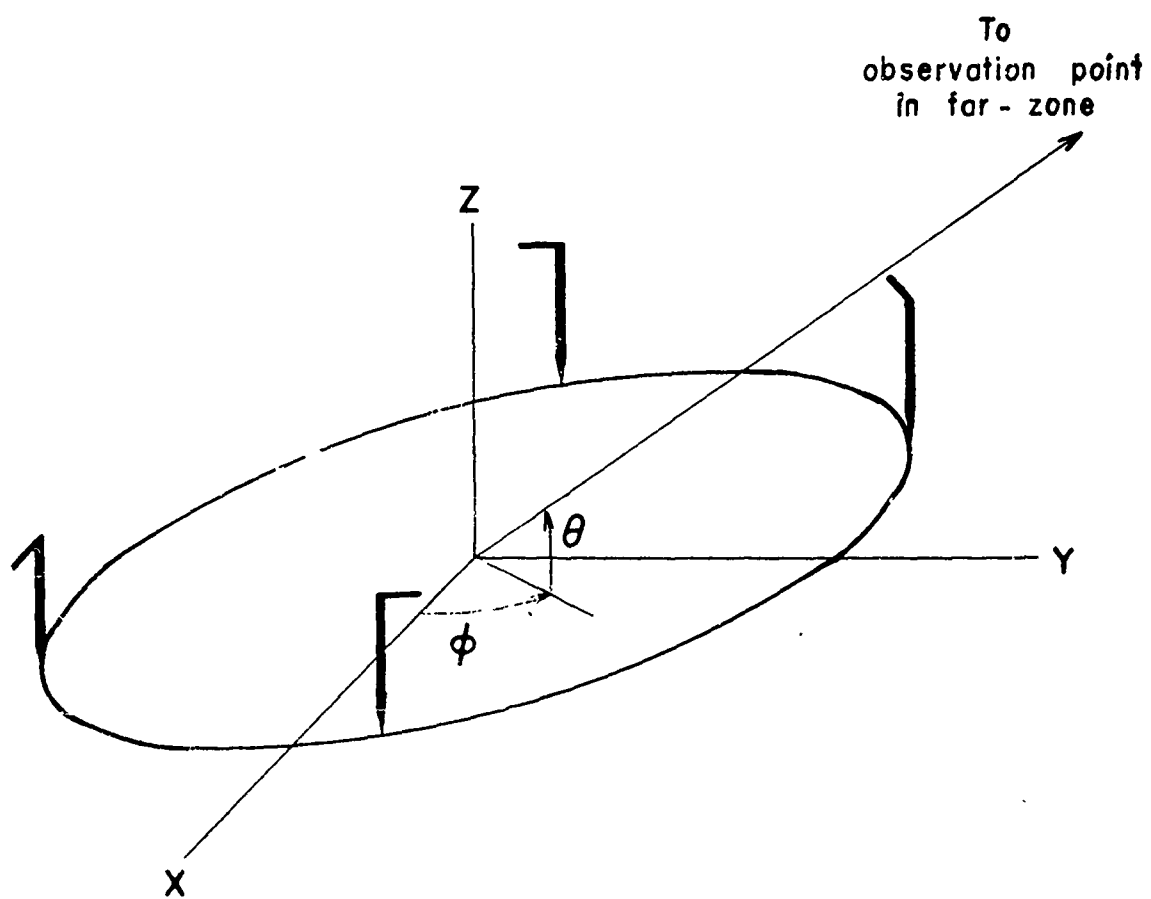
C-18

Fig. 3   Imaging in planes Z = 0 and Y = 0.

Fig. 4   Ring Array of Antenna Elements.

APPENDIX D

INSTRUCTIONS FOR USE OF PROGRAM "PLOTPAT"
(A Supporting Program for Program "WIRTNA")

Control Data 3800 Version

Program PLOTPAT is used to plot antenna patterns using the

pattern data generated by the linear antenna program WIRTNA. The

pattern data are punched on data cards in a very compact form by

WIRTNA. These cards are read by a subroutine BYNIN in program

PLOTPAT along with other data cards which indicate the particular

pattern to be plotted. PLOTPAT is written quite generally, and any

azimuth or elevation pattern cut may be chosen. Program PLOTPAT

executes on the CDC 3800 and places the pattern plotting instructions

on a magnetic tape. The instructions on this magnetic tape are then

read by the CDC 160 A computer which drives the California Computer

Products plotter (CDC Model 165).

DESCRIPTION OF CARD INPUT

```
400      ID = 0
         IW = 0

 20      READ 1, (TITLE(I), I = 1, 10), MODE
         IF (TITLE(1)-1H ) 30, 100, 30

 30      ID = ID + 1
         READ 2, IGROUND, EREF(ID), NANG(1, ID), ANGSTAR(1, ID),
         ANGSTEP(1, ID), NANG(2, ID), ANGSTAR(2, ID), ANGSTEP(2, ID)

         CALL BYNIN(  , P(IW+1), NWORDS(ID)
         IW = IW+1
         GO TO 20
```

C ONE BLANK IS READ AFTER BINARY DATA DECK READ   BY BYNIN
  IN ORDER TO GET TO STATEMENT 100

```
100      READ 3, BOTTOM, NCIRCLE

110      READ 4, TITL, PATTYPE, ANGLE, BNDANGL, BNDANGU,
         ITYPE, ICONTINU
```

C AN UNLIMITED NUMBER OF TITL PATTYPE CARDS MAY BE READ IN
  SERIES

C IN ORDER TO GET FROM STATEMENT 110 TO 100, READ 6HNEWBOT
  INTO TITLE.

C IN ORDER TO END ALL PLOTTING, READ 3HEND INTO TITLE.

C IN ORDER TO READ NEW PATTERN DATA FROM ANOTHER BINARY DECK
  READ A BLANK INTO TITL.

FORMAT STATEMENTS

```
1      FORMAT (9A8, A4, I4)

2      FORMAT ( I5, E15.5, 2(I5, 2F10.5))

3      FORMAT (F10.4, 3I10)

4      FORMAT (A8, 2X, A2, 8X, 3F10.4, 2I10)
```

D-2

An explanation of the symbols used in these statements follows:

TITLE   is read from the first card of each binary data deck to
                     identify the case.

MØDE   is the order of the ring array mode.

IGRØUND   If IGRØUND = 1, the ground is present; if IGRØUND = 0,
                     no ground.

EREF   a normalization factor, gain = E /EREF.

NANG(1, I)   number of elevation angles.

NANG(2, I)   number of azimuth angles.

NWØRDS(I)   4. 0*NANG(1, I)*NANG(2, I) .

ANGSTAR(1, I)   the first elevation angle for which pattern data is punched
                     on the data deck .

ANGSTEP(1, I)   the increment in elevation angle.

ANGSTAR(2, I)   the first azimuth angle for which pattern data is punched
                     on the data deck .

ANGSTEP(2, I)   the increment in azimuth angle.

P   an array in which the pattern data is stored. The total
                     number of words available in this array is 12 102 words.

BØTTØM   the lowest DB value on the DB plot; otherwise BOTTOM
                     is meaningless.

NCIRCLE = 1   then plot the unity gain circle.

NCIRCLE = 0   then normalize pattern to unity and do not plot the circle.

PATTYPE   is a Hollerith constant determining whether an elevation
                     or azimuth cut is to be plotted.

PATTYPE = EL   then plot pattern versus elevation at an azimuth
defined by ---angle.

PATTYPE = AZ   then plot pattern versus azimuth at an elevation
defined by ---angle.

PLOT PATTERNS BETWEEN BANANGL AND BANANGU (DEG.)

ITYPE   determines the type of pattern plot.

ITYPE = 1   power plot.

ITYPE = 2   DB plot

ITYPE = 3   AMP plot.

ITYPE = 4   AMP plot of major and minor axes in place of THETA
and PHI comp.

ICONTINUE   makes it possible to plot several curves on one graph.

ICONTINU = 1   then add to the previous plot

DOCUMENT CONTROL DATA - R & D

(Security classification of title, body of abstract and indexing annotation must be entered when the overall report is classified)

1. ORIGINATING ACTIVITY *(Corporate author)*	2a. REPORT SECURITY CLASSIFICATION
TRG/Division of Control Data Corporation 535 Broad Hollow Rd, Melville, N.Y. 11746	Unclassified
	2b. GROUP

3. REPORT TITLE

INVESTIGATION OF GENERAL WIRE ANTENNAS

4. DESCRIPTIVE NOTES *(Type of report and inclusive dates)*

Final Report - May 1966 to July 1967

5. AUTHOR(S) *(First name, middle initial, last name)*

Mogens G. Andreasen
Robert L. Tanner

6. REPORT DATE	7a. TOTAL NO. OF PAGES	7b. NO. OF REFS
August 1967	82	16

8a. CONTRACT OR GRANT NO	9a. ORIGINATOR'S REPORT NUMBER(S)
DA 28-043 AMC-02373(E)	W-127
b. PROJECT NO. 1P6-20501-A448	
c. Task-04	9b. OTHER REPORT NO(S) *(Any other numbers that may be assigned this report)*
d. Subtask-05	ECOM-02373F

10. DISTRIBUTION STATEMENT

Each transmittal of this document outside the agencies of the U.S. Government must have prior approval of CG, U.S. Army Electronics Command, Fort Monmouth, N.J.

11. SUPPLEMENTARY NOTES	12. SPONSORING MILITARY ACTIVITY
	U.S. Army Electronics Command Fort Monmouth, New Jersey 07703 AMSEL-NL-R-1

13. ABSTRACT

Integral equations for the current distribution on an arbitrary wire antenna have been programmed for a digital computer. The resulting computer program will calculate the current distribution, the input impedance, and the radiation pattern of a wire antenna of arbitrary geometry. Considered as a transmitting antenna, the antenna is excited by electromotive forces applied in any number of gaps along the wires. The program developed will permit these gaps to be connected by an arbitrary non-radiating network, and it will take into account resistive and reactive loading along the wires. The program will also treat the antenna as a receiving antenna, if desired, and then uses a distant dipole as the source of the induced current distribution. The numerical integral equation method used is essentially an exact method. The principal errors in the calculations arise in the numerical integration of the integrals in the integral equations, and these errors can be controlled. It is usually quite easy to obtain accuracies far better than normal measurement accuracies, and at a much lower cost.

DD FORM 1473 NOV

KEY WORDS	LINK A		LINK B		LINK C	
	ROLE	WT	ROLE	WT	ROLE	WT
Antennas, Wire, Calculations						
Wire Antennas, general calculations						

13. ABSTRACT (cont)

Numerical results are presented for a simple dipole, a Yagi antenna array, a log-periodic antenna array, an airplane tail-cap antenna, a center-fed whip antenna, and a compact VHF antenna. Most results have been verified by measurements.

SUPPLEMENTARY

INFORMATION

TAB No. 69-22   15 November 1969

IDENTIFICATION	FORMER STATEMENT	NEW STATEMENT	AUTHORITY
AD-819 198L TRG Inc., Melville, N. Y. Final rept. May 66-Jul 67. Rept. no. TRG-W-127-F, ECOM-02373-F Aug 67 Contract DA-28-043-AMC-02373(E)	USGO: others to Commanding General, Army Electronics Command, Attn: AMSEL-NL-R-1, Fort Monmouth, N. J.	No limitation	USAEC ltr, 15 Jul 69